

AD-A087 476

ILLINOIS UNIV AT URBANA-CHAMPAIGN ELECTROMAGNETICS LAB  
EVALUATION OF LOSSES IN MICROSTRIP ANTENNA MATERIALS. (U)  
APR 80 Y T LO, W F RICHARDS, J E BREWER F19628-7

**F/G 9/5**

F19628-78-C-0025

UNCLASSIFIED

**RADC-TR-80-85**

NL

$$I_{\text{eff}} = I_{\text{eff}}^{\text{eff}} + I_{\text{eff}}^{\text{eff}}$$

24

END

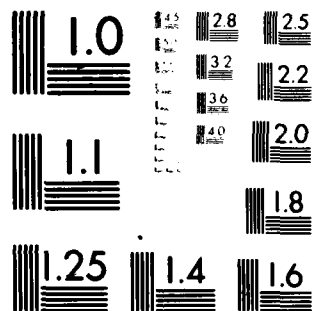
DATE \_\_\_\_\_

FILED

88

BTIC





MICROCOPY RESOLUTION TEST CHART  
NATIONAL BUREAU OF STANDARDS-1963-A



**RADC-TR-80-85**

**Interim Report**

**April 1980**

LEVEL II



# **EVALUATION OF LOSSES IN MICROSTRIP ANTENNA MATERIALS**

**University of Illinois at Urbana Champaign**

Y. T. Lo  
W. F. Richards  
J. E. Brewer

ADA 087476

APPROVED FOR PUBLIC RELEASE; DISTRIBUTION UNLIMITED

**ROME AIR DEVELOPMENT CENTER  
Air Force Systems Command  
Griffiss Air Force Base, New York 13441**

**DTIC  
ELECTE  
AUG 4 1980  
S D**

80 8 1 054



This report has been reviewed by the RADC Public Affairs Office (PAO) and is releasable to the National Technical Information Service (NTIS). At NTIS it will be releasable to the general public, including foreign nations.

RADC-TR-80-85 has been reviewed and is approved for publication.

APPROVED:

*John A. Strom*

JOHN A. STROM  
Antennas and RF Components Branch  
Electromagnetic Sciences Division

APPROVED:

*Allan C. Schell*

ALLAN C. SCHELL, Chief  
Electromagnetic Sciences Division

FOR THE COMMANDER:

*John P. Huss*

JOHN P. HUSS  
Acting Chief, Plans Office

If your address has changed or if you wish to be removed from the RADC mailing list, or if the addressee is no longer employed by your organization, please notify RADC (EEA) Hanscom AFB MA 01731. This will assist us in maintaining a current mailing list.

Do not return this copy. Retain or destroy.



UNCLASSIFIED

SECURITY CLASSIFICATION OF THIS PAGE (When Data Entered)

REPORT DOCUMENTATION PAGE		READ INSTRUCTIONS BEFORE COMPLETING FORM	
1. REPORT NUMBER RADCR-80-85	2. GOVT ACCESSION NO. AD-A087476	3. RECIPIENT'S CATALOG NUMBER (9)	
4. TITLE (and Subtitle) EVALUATION OF LOSSES IN MICROSTRIP ANTENNA MATERIALS.		5. TYPE OF REPORT & PERIOD COVERED Interim Report #3 no. 3	
6. AUTHOR(s) Y. T./Lo J. E./Brewer W. F./Richards		7. PERFORMING ORG. REPORT NUMBER N/A	
8. CONTRACT OR GRANT NUMBER(s) F19628-78-C-0025		9. PROGRAM ELEMENT, PROJECT, TASK AREA & WORK UNIT NUMBERS 61102F 2305J323	
10. CONTROLLING OFFICE NAME AND ADDRESS University of Illinois at Urbana-Champaign Dept of Electrical Engineering/Electromagnetics Laboratory, Urbana IL 61801		11. REPORT DATE Apr 1980	
12. CONTROLLING OFFICE NAME AND ADDRESS Deputy for Electronic Technology (RADCR/EEA) Hanscom AFB MA 01731		13. NUMBER OF PAGES 53	
14. MONITORING AGENCY NAME & ADDRESS (if different from Controlling Office) Same		15. SECURITY CLASS. (of this report) UNCLASSIFIED	
16. DISTRIBUTION STATEMENT (of this Report) Approved for public release; distribution unlimited.		17. SECURITY CLASS. (of the abstract entered in Block 20, if different from Report) Same	
18. SUPPLEMENTARY NOTES RADCR Project Engineer: John A. Strom (EEA)			
19. KEY WORDS (Continue on reverse side if necessary and identify by block number) Microstrip antennas; dielectric and copper loss			
20. ABSTRACT (Continue on reverse side if necessary and identify by block number) A microstrip antenna consists of a conducting patch etched on a dielectric substrate over a ground plane. To evaluate the antenna efficiency, one must know the losses in the material. The dielectric loss is specified by its loss tangent and the copper by its conductivity (or equivalently by its skin-depth at a given frequency). Usually, they can be determined separately with well-known experimental procedures. However, for the copper-cladded material used in microstrip			

DD FORM 1473

JAN 73

EDITION OF 1 NOV 65 IS OBSOLETE

UNCLASSIFIED

SECURITY CLASSIFICATION OF THIS PAGE (When Data Entered)

408102 2/4



UNCLASSIFIED

SECURITY CLASSIFICATION OF THIS PAGE(When Data Entered)

antennas, the surfaces of both the dielectric slab and copper (20) plates are deliberately roughened and filled with bonding agent in-between for mechanical strength. In this case, the separate measurements for the two materials become meaningless.

Taking advantage of the fact that the dielectric loss is proportional to the volume of a cavity, whereas the copper loss is proportional to the surface area, it is possible to separate the two losses by measuring samples of various thicknesses. Many measurements were conducted in this manner, and in most cases good consistent results were obtained. The loss parameters so determined resulted in theoretically computed antenna impedance characteristics in nearly perfect agreement with the measured results. However, the inconsistency in a few other cases suggests that there may be a significant amount of inhomogeneity in the manufacturing process in the material from one part to the other, or from batch to batch.

Accession For	
NTIS GRA&I	<input checked="checked" type="checkbox"/>
DDC TAB	<input type="checkbox"/>
Unannounced	<input type="checkbox"/>
Justification	
By _____	
Distribution/	
Availability Codes	
Dist.	Avail and/or special
A	

UNCLASSIFIED

SECURITY CLASSIFICATION OF THIS PAGE(When Data Entered)



## TABLE OF CONTENTS

I.	INTRODUCTION .....	1
II.	REVIEW OF METHODS .....	3
III.	MEASUREMENT METHOD AND CONSIDERATIONS .....	7
	A. Measurement Choice .....	7
	B. Measurement Procedure .....	8
	C. Relationship of Q to Loss Tangent and Skin Depth .....	17
IV.	RESULTS .....	26
	A. Results for Rexolite 2200 .....	26
	B. Results for Duroide 5880 .....	40
V.	DISCUSSION .....	43
	A. Self Consistency.....	43
	B. Measurement Error Reduction.....	44
	C. Air Gaps.....	44
	D. End Walls.....	45
	E. Feed Point .....	46
	F. Time, Moisture, and Temperature.....	47
	G. Mode Approximation .....	47
	H. Solid Cavity.....	47
	I. Reducing Solution Area.....	48
VI.	CONCLUSION .....	50
	REFERENCES .....	51
	APPENDIX .....	52



## LIST OF FIGURES

Figure	Title	Page
1	Microstrip Antenna (Rectangular)	1
2	Equipment Set Up	9
3a	Impedance Plot	10
3b	Circuit Model of Cavity	12
4	Impedance Plot With Coupling Losses	15
5	Circuit Model of Cavity	15
6	Cavity Geometry	18
7	Cavity Side View	19
8	Cavity Coordinates	21
9	Cavity Q	27
10	Solution Methods Plot	29
11a-m	Solution Plot	31-37
12	Skin Depth Solution	38
13	Loss Tangent Solution	38
14	Conductivity Solution	38
15	Solution Plot	42
16	Edge Construction	45
17	Feed Line	46
18	Solution Plot	49
19	r-Plane	53



## LIST OF TABLES

Table	Title	Page
1	Solution Results	30



## CHAPTER 1

## INTRODUCTION

A microstrip antenna is made of a ground plane, an antenna element above the ground plane, and a dielectric sheet separating these two conductors. A diagram of a microstrip antenna is shown in Figure 1. In this report tests on two different materials were performed. They were double-sided copper-clad, Rexolite 2200 and Duroid 5880.

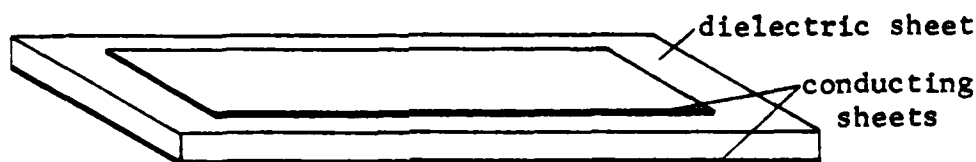


Figure 1 MICROSTRIP ANTENNA (RECTANGULAR)

The losses in the microstrip antenna come from two sources; the losses in the dielectric (loss tangent) and the losses in the conducting sheets (conductivity). In this report a measurement procedure is presented that will separate these two sources.



The procedure used cavities constructed from the antenna materials. The antenna material was cut into rectangular pieces and copper foil was soldered around the edges of the two copper-cladding sheets. Closing off the edges removed the radiation loss. The  $Q$  of these cavities were measured. The loss components of the dielectric and conducting sheets are related by  $\frac{1}{Q} = \frac{1}{Q_D} + \frac{1}{Q_C}$ , where  $Q_D$  and  $Q_C$  are the  $Q$  factors associated with the loss components of the dielectric and conducting sheets respectively. Since the dielectric loss is dependent on the thickness of the dielectric, the two losses can be separated by constructing two cavities of the same length and width, but of different thicknesses, and measuring the  $Q$ . With the measured  $Q$  and the thicknesses of the cavities known the problem was reduced to a linear problem of two equations for the two unknowns.



## CHAPTER 2

## REVIEW OF METHODS

There are different methods available to measure the loss tangent of dielectrics [2]. In one group of methods the dielectric sample is fitted into a waveguide and the reflected or transmitted waves are measured. In another, comparison of resonant behavior is made for cavities with and without dielectric samples in them.

One method using waveguide views the sample of dielectric in the waveguide as a two-port device. Usually this method involves placing a dielectric sample at the end of a short circuited waveguide and then placing it one quarter wavelength from the short. In this way one can measure the short circuit and open circuit admittances (impedances) and deduce the complex dielectric constant of the sample.

Another method using waveguide compares two short-circuited waveguides, one with a dielectric sample at the end and the other without. Measurements of the difference in voltage minimum positions in the slotted line and the VSWR of the line with and without the sample are taken. The complex dielectric constant can then be computed by solving a transcendental equation.



There is another method using waveguide that does not require special equipment or a solution of a transcendental equation, but this method is generally less accurate. This method also uses a short-circuited line but the dielectric sample is placed at different distances from the short. Only the simplest equipment is required for measuring the distance change in voltage minima and the VSWR. With this information the complex dielectric constant can also be calculated.

The methods, including fitting the dielectric sample into waveguide, would also apply to coaxial line. Problems with these waveguide methods are (1) obtaining special measuring equipment, (2) solving a transcendental equation, (3) having inaccuracies, (4) preparing tight fitting dielectric samples for insertion in the waveguide, and (5) obtaining all the waveguide required for measurement at the required frequencies. While these methods can give good results for the dielectric losses, none is applicable for copper-cladded material used for microstrip antennas due to the presence of the bonding agent and surface roughness in the material which cannot be separated from the copper but can introduce substantial loss.

Dielectric measurement methods using cavities involve the comparison of cavities with dielectric samples in them to a reference cavity. The test cavity has a dielectric sample that partially or completely fills the cavity and the reference



cavity is empty or is filled with a dielectric with known properties. The complex dielectric constant can be determined by measuring the  $Q$  and the resonant frequency of the cavity. The copper loss in the walls can be determined by measuring the  $Q$  of the cavity with the dielectric removed.

These cavity methods could be modified to measure the losses in the dielectric and the copper conductors of microstrip antennas. One of the most significant problems with cavity methods is the large frequency excursion caused by comparing an empty cavity to a cavity filled with a dielectric sample. The large frequency excursion could cause inaccuracies in measurements. This problem could be alleviated by using a reference dielectric in the test cavity. This reference dielectric should have a dielectric constant close to the dielectric constant to be measured to minimize the frequency excursion. Another significant problem is the need of rigid cavities of the appropriate dimensions for measurement at the required frequencies. Finally, the most serious problem is that in the copper-cladded dielectric material, which is used exclusively for microstrip antennas, the bonding agent between copper and dielectric as stated before can introduce substantial loss. Thus an empty cavity reference measurement could not give correct information on dielectric loss tangent.



Sato, in his dielectric measurement, [3] uses microstrip line. It involves comparing measurements of a microstrip line to that line with a test dielectric sample clamped on top of the line. This method gives good results for the real part of the dielectric constant but poor results for the loss tangent. Of course, this method cannot give an accurate measurement of copper loss either.

In this thesis an attempt is made to devise a new measurement method which would separate the dielectric loss from the copper loss including that of the bonding material.



## CHAPTER 3

## MEASUREMENT METHOD AND CONSIDERATIONS

## A. MEASUREMENT CHOICE

The method chosen and developed in this report uses multiple thickness cavities to separate the copper losses and dielectric losses. The copper loss (conductivity) is related to the skin depth and the dielectric loss is described in terms of loss tangent. The skin depth ( $\Delta$ ) and the loss tangent ( $\tan\delta$ ) are linearly related to the  $Q^{-1}$  of the cavity. By using two cavities of different thickness and measuring the  $Q$  of the cavities, a solution can be obtained for the loss tangent ( $\tan\delta$ ) and skin depth ( $\Delta$ ). If the dielectric constant was not known it could easily be determined from the dimensions and resonant frequency of the cavity.

This method was investigated because it requires no special test fixture, the cavity is made of the same material as the microstrip antenna, the measurements are straightforward and the calculations are simple.



## B. MEASUREMENT PROCEDURE

Determination of cavity size was the first step in the measurement procedure. The size of the cavity was determined by the resonant frequency at which the measurement was made. The dimensions (length and width) were found by the formula to determine cutoff frequency in a waveguide [6] :

$$f_r = \frac{c}{2 \pi \sqrt{\epsilon_r}} \sqrt{\left(\frac{m \pi}{a}\right)^2 + \left(\frac{n \pi}{b}\right)^2} \quad (3.1)$$

The symbols m & n are the mode numbers and the symbols a & b are the length and width. The double-clad boards were cut to the desired size. One board was used as a single thickness cavity. Two other boards had the copper removed from one side then put together to make a double thickness cavity. Later a third board was stripped on both sides and put in the center of the double thickness cavity to make a triple thickness cavity. These cavities were closed in by soldering copper tape around the edges. The multiple layer cavities were clamped to remove the air and ensure correct thickness. The cavities were fed by semi-rigid coax connected to both sides through the board.

The Q of each cavity was determined by the impedance method [1] . A network analyzer test set-up was used to measure the impedance of each cavity. The half-power points



in frequency ( $f_1$ ,  $f_2$ ) and the resonant frequency point ( $f_0$ ) were determined from the measured impedance. These frequency points were used to find Q by using the relationship  $Q = f_0 / (f_1 - f_2)$  [2].

The equipment used to measure the impedance of the cavities consisted of a network analyzer, plotter, frequency counter, and sweep frequency generator, as set up in Figure 2.

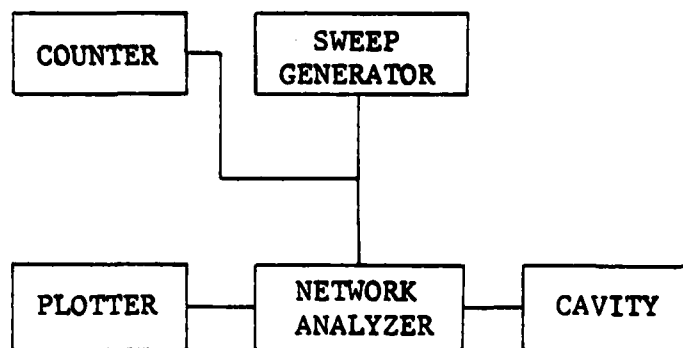


Figure 2 Equipment Set Up

Two procedures were used to find the Q from the impedance. Both of the procedures used the network analyzer. The first, which is more accurate [1], locates frequencies where  $R = X$ , (the real part equal to the imaginary part). This is an easy procedure that is limited to cases of negligible loss in the feed to the cavity (coupling loss). Most of the cavities had negligible coupling loss. The second method, which is easily adapted to account for coupling loss, involves measuring VSWR.



The first procedure to find  $Q$  was aided by using a plotter connected to the network analyzer. On the plotter was a Smith chart with  $R = X$  and  $\pm B = G + 1$  construction lines drawn in as in Figure 3a. These lines were used to find the unloaded  $Q$  ( $Q_0$ ) and the loaded  $Q$  ( $Q_L$ ). The unloaded  $Q_0$  is the  $Q$  of the cavity, the loaded  $Q_L$  is the  $Q$  of the system, which includes the coupling loss.

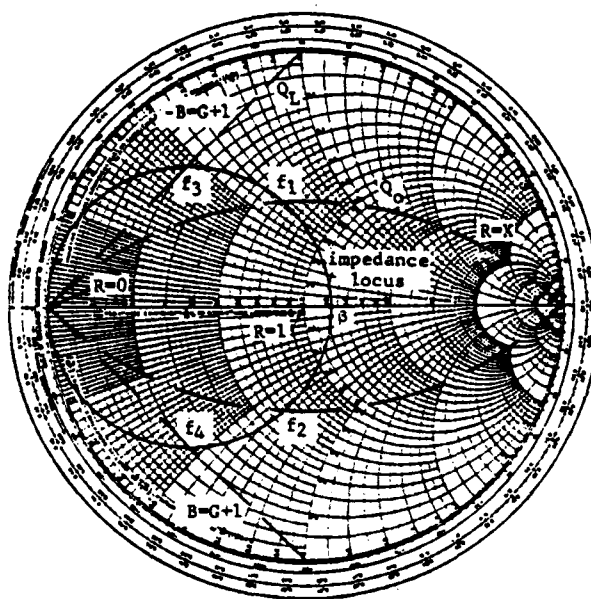


Figure 3a Impedance Plot

The detuned short position was first found on the left side of the chart where  $R = 0$ . When the frequency was swept through resonance the impedance locus was displayed as in Figure 3a. The resonant point is on the real axis. At the half power frequency points the impedance is on the  $R = X$  line.



$Q_o$  was found from the half-power frequencies. For the loaded Q-factor,  $Q_L$ , the source impedance (assuming matched) is included and the half-power points are given by the intersections of the impedance locus and the lines  $\pm B = G + 1$  in the Smith chart. From  $Q_L$ ,  $Q_o$  could also be determined by the relationship  $Q_o = (1 + \beta) Q_L$ , where  $\beta$  is the coupling parameter shown in Figure 3a.

This method for determining Q was based on representing the cavity as a lumped circuit. The admittance of a parallel RLC circuit is

$$Y = G + j(\omega C - 1/\omega L) \quad (3.2)$$

and resonance frequency  $\omega_o = 1/\sqrt{LC}$ . Then at  $\omega$

$$\begin{aligned} Y &= G + j \omega_o C \left( \frac{\omega}{\omega_o} - \frac{1}{\omega \omega_o LC} \right) \\ &= G + j \omega_o C \left( \frac{\omega}{\omega_o} - \frac{\omega_o}{\omega} \right) \end{aligned}$$

Since the resonant Q,  $Q_o = \frac{\omega_o C}{G}$

$$\begin{aligned} Y &= G + jB \\ Y &= G \left[ 1 + jQ_o \left( \frac{\omega}{\omega_o} - \frac{\omega_o}{\omega} \right) \right] \\ &= G \left[ 1 + jQ_o \frac{\omega^2 - \omega_o^2}{\omega \omega_o} \right] \end{aligned}$$



$$\begin{aligned}
 &= G \left[ 1 + jQ_0 \left( 2\delta + \frac{\omega}{\omega_0} \delta^2 \right) \right] \\
 &\approx G \left[ 1 + j2\delta Q_0 \right] \text{ for } |\delta| \ll 1
 \end{aligned} \tag{3.3}$$

where  $\delta = (\omega - \omega_0)/\omega$

The amplitude of the voltage in the circuit was given by  $I/|Y|$  and was therefore proportional to:

$$\frac{G}{|Y|} = \frac{1}{\sqrt{1 + Q_0^2 \left[ \omega/\omega_0 - \omega_0/\omega \right]^2}} \approx \frac{1}{\sqrt{1 + (2\delta Q_0)^2}} \tag{3.4}$$

When  $Q_0^2 (\omega/\omega_0 - \omega_0/\omega)^2 = 1$  or  $2\delta Q_0 \approx 1$  the susceptance equals the conductive ( $G = \pm B$ ), the amplitude of the current dropped to  $1/\sqrt{2}$  of its value at resonance, and the power dissipated was halved. Let  $2\delta f = \Delta f =$  "half-power bandwidth" (3.5)

then

$$Q_0 = f_0 / \Delta f = f_0 / (f_1 - f_2). \tag{3.6}$$

For the loaded  $Q$  ( $Q_L$ ), the cavity can be represented near resonance by the circuit shown in Figure 3b.

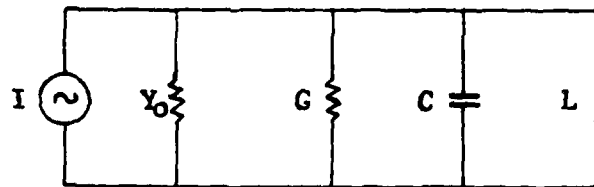


Figure 3b Circuit Model of Cavity



Then

$$Q_L = \frac{\omega_o C}{G + Y_o} = \frac{\omega_o C/G}{1 + (Y_o/G)} = \frac{Q_o}{1 + \beta}$$

where  $\beta$  (coupling parameter) =  $Y_o/G$ . When  $\beta < 1$ ,  $= 1$  and  $> 1$ , the system is said to be undercoupled, critically coupled, and overcoupled respectively. Note that at resonance the admittance of the cavity as seen from Equation (3.2) is  $G$ . Therefore  $\beta = (\text{normalized resonant admittance of the cavity})^{-1} = \text{normalized resonant cavity impedance} = (\text{SWR})^{\pm 1}$  at resonance, where  $\pm 1$  is used if  $\beta \geq 1$  respectively. They can be read directly from the chart. Now the total normalized admittance of the system as viewed by the ideal constant current generator is

$$\begin{aligned} Y_L &= \frac{1}{Y_o} (Y_o + G + jB) = 1 + G_n + jB_n \\ &= (G_n + 1) \left[ 1 + j2Q_L \delta \omega / \omega_o \right] \end{aligned}$$

The half-power frequency occurs when

$$\pm B_n = G_n + 1 \text{ or } \pm \frac{X_n}{R_n^2 + X_n^2} = \frac{R_n}{R_n^2 + X_n^2} + 1$$

$$\text{or } Q_L = \frac{\omega_o}{2 \delta \omega} = \frac{\omega_o}{|\omega_3 - \omega_4|}$$

This implies that  $Q_L$  can be determined by finding the intersection points  $f_3$  and  $f_4$  in frequency of the cavity impedance locus and the lines (See Appendix)  $\pm B_n = G_n + 1$  in the Smith chart



as shown in Figure 3a. Thus from  $Q_L$  and the normalized resonant impedance  $\beta$  one obtains

$$Q_o = (1 + \beta) Q_L$$

where  $\beta$  = normalized cavity resonant impedance.

Another method, which is particularly useful when there is a coupling loss between the transmission line feed and the cavity, is based on the measurement of SWR at resonance and the half-power frequencies.

As discussed in Reference [1], there are in general two convenient equivalent circuit representations for the system, the so-called detuned-short and detuned-open position circuit, depending on which reference plane in the transmission is used. When a high-Q cavity is detuned, its impedance is approximately purely reactive, resulting in a total reflection and perfect standing wave on the line. If the voltage minimum position is taken as the reference plane (called the detuned-short position), the equivalent circuit becomes the generator with internal impedance  $Z_o$  in series with the coupling loss resistance  $R_1$  and a parallel resonant circuit of the cavity. On the other hand at the voltage maximum (the detuned-open position) which is  $\lambda/4$  away from the detuned-short position, the cavity can be represented by a series resonant circuit. Let us consider the former as shown in Figure 4.



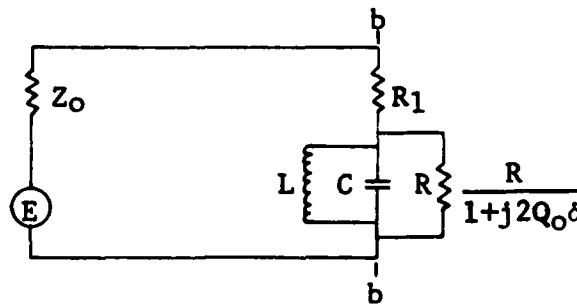


Figure 4 Circuit Model of cavity

The cavity impedance as given by Equation (3.3) is:

$$Z = \frac{R}{1 + j2Q_o \delta} \quad (3.7)$$

However at resonance ( $\delta = 0$ ) the measured impedance at terminals bb must be  $R_1 + R = R_2$  which is shown in Figure 5 as the intersection of the impedance locus with the real axis.

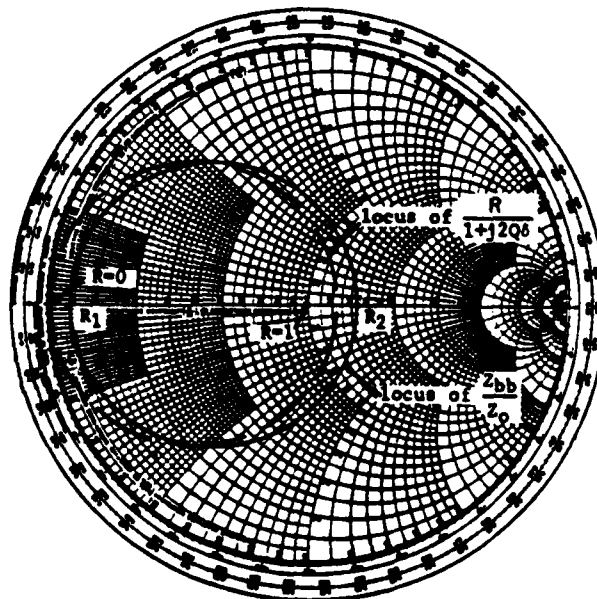


Figure 5 Impedance Plot With Coupling Losses



Thus the observable impedance at bb is

$$Z_{bb} = R_1 + \frac{R}{1 + j2Q_0\delta} \quad (3.8)$$

At half-power points of the cavity impedance

$$2 Q_0 \delta = \pm 1 \quad \text{and}$$

$$Z_{bb} = R_1 + \frac{R}{1 \pm j} \quad (3.9)$$

The SWR at these points

$$(SWR)_{\frac{1}{2}} = \frac{1 + |\Gamma|}{1 - |\Gamma|} = \frac{|Z_{bb} + Z_o| + |Z_{bb} - Z_o|}{|Z_{bb} + Z_o| - |Z_{bb} - Z_o|} \quad (3.10)$$

Let  $\beta = (R + R_1)/Z_o$ ,  $\gamma = R_1/(R + R_1)$ ;

then at a half-power frequency,

$$\frac{Z_{bb}}{Z_o} = \beta \left( \gamma + \frac{1 - \gamma}{1 \pm j} \right)$$

$$\begin{aligned} |1 + Z_{bb}/Z_o| &= |(1 + \beta\gamma)(1 \pm j) + \beta(1 - \gamma)| / \sqrt{2} \\ &= |(1 + \beta) \pm j(1 + \beta\gamma)| / \sqrt{2} \end{aligned} \quad (3.11a)$$

$$\left| 1 - Z_{bb}/Z_o \right|_{\delta=0} = |(1 - \beta) \pm j(1 - \beta\gamma)| / \sqrt{2} \quad (3.11b)$$

and

$$\begin{aligned} (SWR)_{\frac{1}{2}} &= \frac{|(1 + \beta) + j(1 + \beta\gamma)| + |(1 - \beta) + j(1 - \beta\gamma)|}{|(1 + \beta) + j(1 + \beta\gamma)| - |(1 - \beta) + j(1 - \beta\gamma)|} \\ &= \frac{[(1 + \beta)^2 + (1 + \beta\gamma)^2]^{\frac{1}{2}} + [(1 - \beta)^2 + (1 - \beta\gamma)^2]^{\frac{1}{2}}}{[(1 + \beta)^2 + (1 + \beta\gamma)^2]^{\frac{1}{2}} - [(1 - \beta)^2 + (1 - \beta\gamma)^2]^{\frac{1}{2}}} \end{aligned}$$



$$\begin{aligned}
&= \frac{\left\{ \left[ (1 + \beta)^2 + (1 + \beta\gamma)^2 \right]^{\frac{1}{2}} + \left[ (1 - \beta)^2 + (1 - \beta\gamma)^2 \right]^{\frac{1}{2}} \right\}^2}{\left[ (1 + \beta)^2 + (1 + \beta\gamma)^2 \right] - \left[ (1 - \beta)^2 + (1 - \beta\gamma)^2 \right]} \\
&= \frac{2 + \beta^2(1 + \gamma^2) + \left[ 4 + \beta^4(1 + \gamma^4) - 2\gamma\beta^2(4 - \gamma\beta^2) \right]^{\frac{1}{2}}}{2\beta(1 + \gamma)} \quad (3.12)
\end{aligned}$$

The Q was found by the above measurement methods. These methods produced repeatability and agreement within 5 percent range. By repeating these measurements, the range of Q for each cavity was found.

#### C. RELATIONSHIP OF Q TO LOSS-TANGENT AND SKIN-DEPTH

The Q and the thickness of the cavities were used to separate the dielectric loss and copper loss. This was accomplished by graphing the equation for the losses (which is derived later).

$$\frac{1}{Q} = \tan \delta + \frac{\Delta}{t} \quad (3.13)$$

The first term on the right hand side of the equation is the dielectric loss tangent and the second term is due to the copper loss. The symbol t is the thickness of the cavities. The  $\Delta$  in the numerator is the skin depth.

Three sets of lines were plotted for the range of Q for each thickness of cavity. These lines intersected in a common area. That common area was the range of the solution of the problem. The dielectric loss was read from the graph and the conductivity was calculated from [6] :



$$\sigma = \frac{1}{\pi f \mu \Delta^2} \quad (3.14)$$

The results of these measurements are shown in Chapter 4.

Equation (3.13) was derived by considering the field problem of the cavity shown in Figure 6.

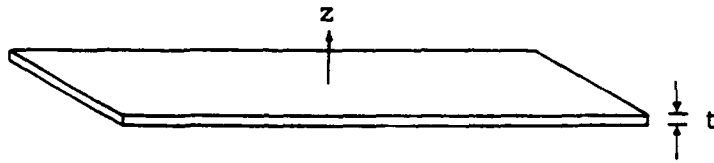


Figure 6 Cavity Geometry

The cavities are thin so the E-field was assumed to be independent of  $z$ . The stored electric and magnetic energy was found to be:

$$W_E = \frac{1}{2} \int_{Vol} \epsilon' |E|^2 dv = \frac{1}{2} t \int_A \epsilon' |E|^2 ds \quad (3.15)$$

$$W_H = \frac{1}{2} \int_{Vol} \mu |H|^2 dv = \frac{1}{2} t \int_A \mu |H|^2 ds \quad (3.16)$$

The power dissipated in the dielectric was found as follows:

$$P_D = \int_{Vol} \bar{J}^* \cdot \bar{E} dv = t \int_A \bar{J}^* \cdot \bar{E} ds \quad (3.17)$$



$$\begin{aligned}
 \epsilon &= \epsilon' - j\epsilon'' \\
 &= \epsilon' (1 - j \tan \delta) \\
 P_D &= \epsilon' \omega t \int_A |E|^2 ds = 2 \omega \tan \delta \left( \frac{t}{2} \int_A \epsilon' |E|^2 ds \right) = (2 \omega \tan \delta) W_E
 \end{aligned}$$

Figure 7 shows the sideview of the cavity with reference axis.

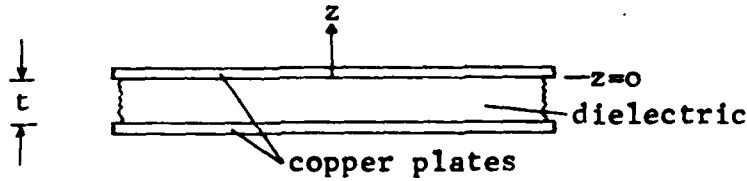


Figure 7 Cavity Side View

The current in the copper was distributed as [6] :

$$J = J_0 e^{-z\gamma} \quad (3.19)$$

where  $\gamma = \sqrt{\omega \mu \sigma / 2} (1+j) = \frac{1}{\Delta} (1+j)$ ,  $\sigma$  = copper conductivity

The total surface current was:

$$J_s = \int_0^\infty J dz = J_0 / \gamma \quad (3.20)$$

then

$$J = \gamma J_s e^{-z\gamma} = \gamma J_s e^{-z(\frac{1}{\Delta} + \frac{j}{\Delta})}$$

and

$$|J| = |\gamma| |J_s| e^{-z/\Delta}$$



Since  $\bar{J} = \sigma \bar{E}$  the power dissipated in both upper and lower plates was found to be [2].

$$\begin{aligned}
 P_C &= 2 \int_0^\infty \int_A \bar{J}^* \cdot \bar{E} \, ds \, dz \\
 &= 2/\sigma \int_0^\infty \int_A |\bar{J}|^2 \, ds \, dz \\
 &= \frac{2}{\sigma} \int_0^\infty \int_A \left| \gamma \int_0^2 J_s \right|^2 e^{-2z/\Delta} \, ds \, dz \\
 &= \frac{4}{\sigma \Delta^2} \int_A \frac{\Delta}{2} \left| \hat{z} \times \bar{H} \right|^2 \, ds \\
 &= \frac{2}{\sigma \Delta} \int_A \left[ |\bar{H}_x|^2 + |\bar{H}_y|^2 \right] \, ds \\
 &= \frac{4}{\sigma \Delta \mu t} \frac{1}{2} t \int_A \mu |\bar{H}|^2 \, ds \\
 &= \frac{4}{\sigma \Delta t \mu} W_H
 \end{aligned}$$

$$\text{thus } P_C = \frac{2\Delta}{t} \omega W_H, \text{ since } \sigma \mu = 2/(\omega \Delta^2) \quad (3.21)$$

At resonance  $W_E = W_H$  therefore the total power dissipated (neglecting side walls) was:

$$P = P_D + P_C = (2 \tan \delta + \frac{2\Delta}{t}) \omega W_E \quad (3.22)$$



Since Q was defined as:

$$Q = 2\pi \frac{\text{total energy stored}}{\text{average power loss per cycle}} = \frac{\omega 2W_E}{(2 \tan\delta + \frac{2\Delta}{t}) \omega W_E}$$

$$= \frac{1}{\tan\delta + (\Delta/t)}$$

This gives Equation (3.13)

A more accurate model which included the side wall losses involved carrying out the integration over the entire cavity surface of Figure 8. This is considered in the following.

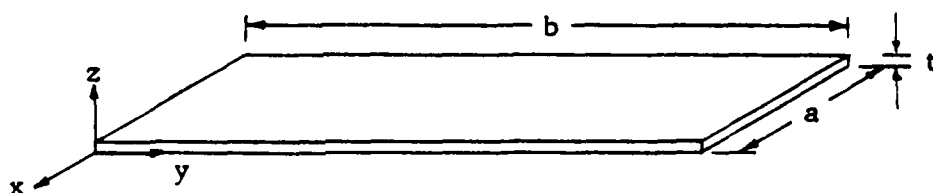


Figure 8 Cavity Coordinates

The total stored energy at resonance ( $W_E = W_H$ ) was

$$W_T = \int_{Vol} \epsilon' |E|^2 dv \quad (3.23)$$



The power dissipated in the dielectric was

$$P_D = \int_{Vol} \omega \epsilon'' |E|^2 dv \quad (3.24)$$

The power dissipated in the copper was:

$$P_C = \int_s \frac{2}{\sigma \Delta} |H_{tan}|^2 ds = \frac{\omega \mu \Delta}{2} \int_s |H_{tan}|^2 ds \quad (3.25)$$

There was no field variation in  $z$ . The fields for the  $m^{th}$  mode were taken to be the same as in a lossless cavity [2]:

$$E_z = \sin \frac{m\pi}{a} x \sin \frac{n\pi}{b} y \quad (3.26a)$$

$$H_x = \frac{j\omega\epsilon}{k_c^2} \left(\frac{n\pi}{b}\right) \sin \frac{m\pi}{a} x \cos \frac{n\pi}{b} y \quad (3.26b)$$

$$H_y = \frac{-j\omega\epsilon}{k_c^2} \left(\frac{m\pi}{a}\right) \cos \frac{m\pi}{a} x \sin \frac{n\pi}{b} y \quad (3.26c)$$

where  $k_c^2 = \left(\frac{m\pi}{a}\right)^2 + \left(\frac{n\pi}{b}\right)^2 = \left(\frac{2\pi}{\lambda_c}\right)^2 = \omega_o^2 \mu\epsilon$ .

Then at resonance

$$\begin{aligned} W_T = 2W_E &= \epsilon' \int_V |E|^2 dv \\ &= \epsilon' \int_0^a \int_0^b \int_0^t \left(\sin \frac{m\pi}{a} x \cos \frac{n\pi}{b} y\right)^2 dx dy dz \\ &= \frac{abte'}{4} \end{aligned} \quad (3.27)$$



and

$$\begin{aligned}
\int_S |H_{\tan}|^2 ds &= 2 \left[ \int_0^t \int_0^b |H_y|_{x=0}^2 dy dz + \int_0^t \int_0^a |H_x|_{y=0}^2 dx dy \right. \\
&\quad \left. + \int_0^a \int_0^b (|H_x|^2 + |H_y|^2) dx dy \right] \\
&= 2 \left( \frac{\omega \epsilon \pi}{k_c} \right)^2 \left[ \left( \frac{n}{b} \right)^2 \frac{at}{2} + \left( \frac{m}{a} \right)^2 \frac{bt}{2} + \left( \frac{n}{b} \right)^2 \frac{ab}{4} + \left( \frac{m}{a} \right)^2 \frac{ab}{4} \right] \\
&= \left( \frac{\omega \epsilon \pi}{k_c} \right)^2 \left[ \frac{n^2 a^3 + m^2 b^3}{a^2 b^2} t + \frac{n^2 a^2 + m^2 b^2}{2ab} \right] \\
&= \left( \frac{\omega \epsilon \pi}{k_c} \right)^2 \left[ 2 \frac{n^2 a^3 + m^2 b^3}{ab} t + (n^2 a^2 + m^2 b^2) \right] \frac{1}{2ab} \\
&= \frac{\epsilon \pi^2}{\mu k_c^2} \left[ 2 \frac{n^2 a^3 + m^2 b^3}{ab} t + (n^2 a^2 + m^2 b^2) \right] \frac{1}{2ab} \\
&= \frac{\epsilon}{\mu} \frac{a^2 b^2}{m^2 b^2 + n^2 a^2} \left[ 2 \frac{n^2 a^3 + m^2 b^3}{ab} t + (n^2 a^2 + m^2 b^2) \right] \frac{1}{2ab} \\
&= \frac{\epsilon}{\mu} \frac{ab}{2} \left[ 2 \frac{n^2 a^3 + m^2 b^3}{ab(n^2 a^2 + m^2 b^2)} t + 1 \right] \quad (3.28)
\end{aligned}$$

Then from Equation (3.25)

$$\begin{aligned}
P_c &= \frac{\omega \mu \Delta}{2} \int_S |H_{\tan}|^2 ds \\
&= \frac{\omega \epsilon \Delta}{2} \frac{ab}{2} \left[ 2 \frac{(n^2 a^3 + m^2 b^3)}{ab(n^2 a^2 + m^2 b^2)} t + 1 \right] \quad (3.29)
\end{aligned}$$



Therefore

$$\begin{aligned}
 \frac{1}{Q} &= \frac{P_D + P_C}{\omega W_T} = \frac{(\omega \tan \delta) W_T}{\omega W_T} + \frac{P_C}{\omega W_T} \\
 &= \tan \delta + \frac{\omega \epsilon \Delta \frac{ab}{4} \left[ 2 \frac{n^2 a^3 + m^2 b^3}{ab(n^2 a^2 + m^2 b^2)} t + 1 \right]}{\frac{\omega ab t \epsilon'}{4}} \\
 &= \tan \delta + \frac{\Delta}{t} \left[ 2t \frac{n^2 a^3 + m^2 b^3}{ab(n^2 a^2 + m^2 b^2)} + 1 \right] \quad (3.30)
 \end{aligned}$$

Equations (3.13) and (3.30) have been used to separate the losses in the dielectric ( $\tan \delta$ ) and losses in the copper ( $\sigma$ ). The first is the simplest and the last is the more accurate. This last formula can be simplified by calculating for the lowest mode as:

$$\frac{1}{Q} = \tan \delta + \frac{\Delta}{t} \left[ \frac{2t \left( \frac{b}{a^2} + \frac{a}{b^2} \right)}{\frac{b}{a} + \frac{a}{b}} + 1 \right] \quad (3.31)$$

Because the thickness,  $t$  is small for this type of antenna the term

$$\frac{2t \left( \frac{b}{a^2} + \frac{a}{b^2} \right)}{\frac{b}{a} + \frac{a}{b}} + 1$$

is typically 1.011 to 1.084 so the formula can be simplified further to



$$\frac{1}{Q} \approx \tan \delta + \frac{\Delta}{t}$$

which is the same as Equation (3.13).

The results for these formulas are presented in the following chapter.



## CHAPTER 4

## RESULTS

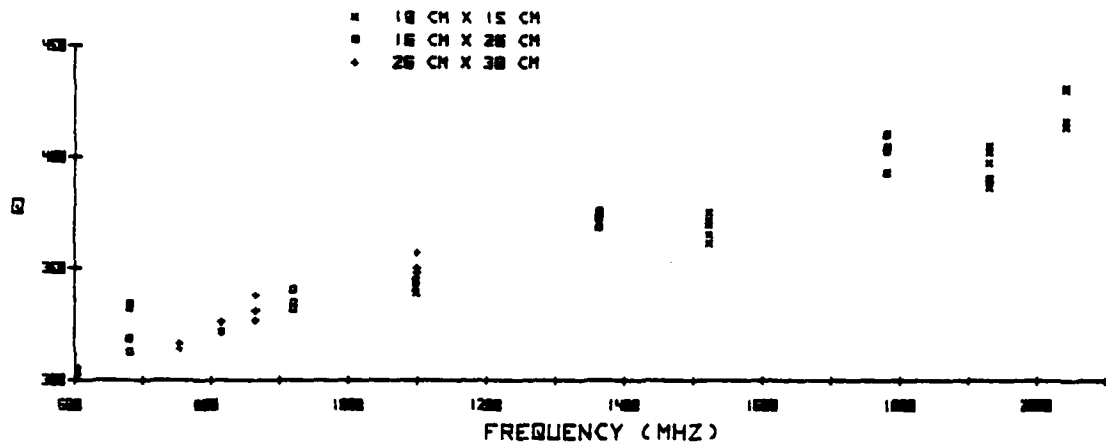
## A. RESULTS FOR REXOLITE 2200

Q was measured for three microstrip cavities of different thicknesses ( $1/16''$ ,  $1/8''$ ,  $3/16''$ ). The Q was measured over a frequency range of 600 MHz to 2 GHz. Measurements over this range of frequencies were accomplished by using sets of cavities of different dimensions (length and width) and resonating these cavities in various modes. The cavity dimensions used were  $10\text{ cm} \times 15\text{ cm}$ ,  $16\text{ cm} \times 26\text{ cm}$ , and  $26\text{ cm} \times 38\text{ cm}$ . These dimensions were chosen because these cavities had resonances that were not overlapping with their other resonances and there was a sufficient number of resonances throughout the required frequency band.

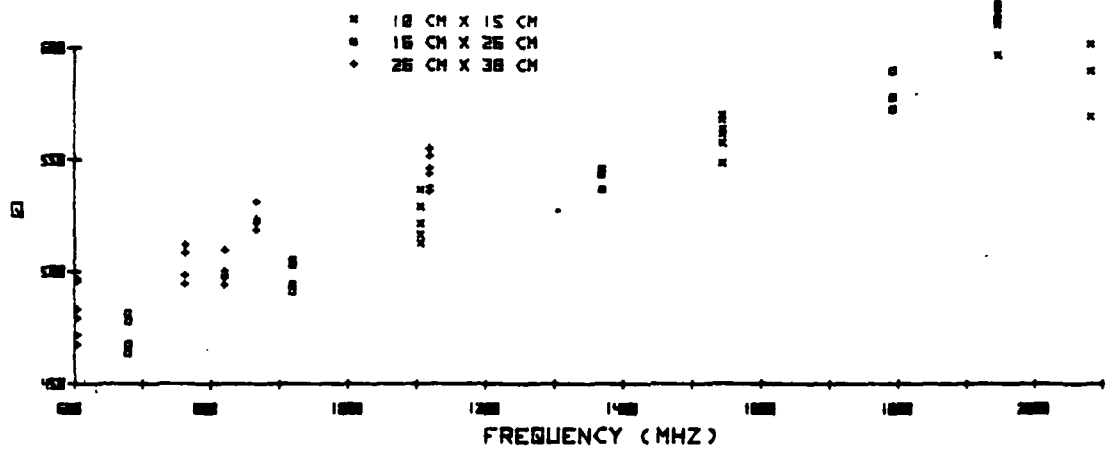
The repeatability of these Q measurements was generally about 5%. This gave a small range of Q rather than a specific value of Q. The results for the Q measurements are in Figure 9. These plots present Q vs. frequency and indicate which cavity it was measured on.



## Q VS. FREQUENCY FOR 1/16 IN CAVITIES



## Q VS. FREQUENCY FOR 1/8 IN CAVITIES



## Q VS. FREQUENCY FOR 3/16 IN CAVITIES

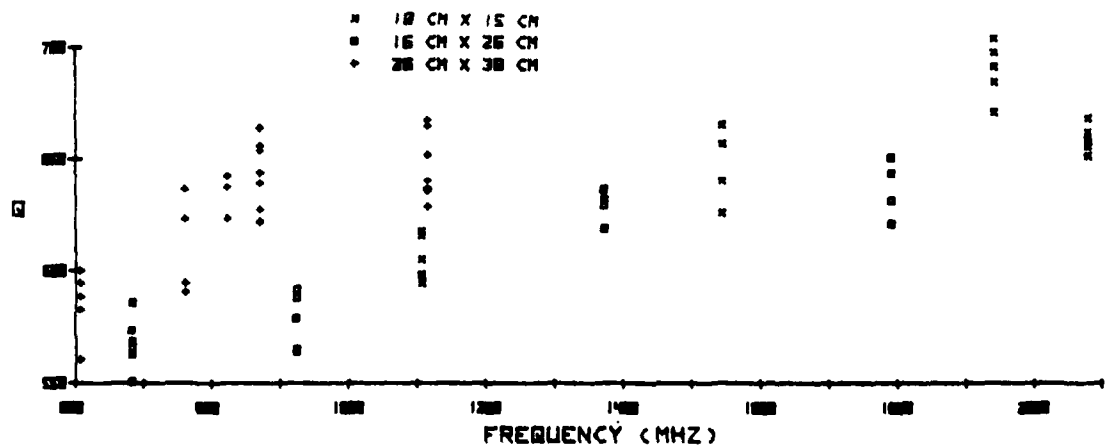


Figure 9 Cavity Q



The comparison of methods for separating the loss tangent and skin depth are presented in Figure 10. These plots were constructed by plotting in dashed lines

$$\frac{1}{Q} = \tan \delta + \frac{\Delta}{t} \quad (4.1)$$

and in solid lines

$$\frac{1}{Q} = \tan \delta + \frac{\Delta}{t} \left[ \frac{2t(n^2 a^3 + m^2 b^3)}{ab(n^2 a^2 + m^2 b^2)} + 1 \right] \quad (4.2)$$

The three sets of lines are from the three thicknesses of the cavities. The steepest slopes are from the thinnest (1/16") cavity and the least steep set of lines is from the thickest (3/16") cavity. The minimum and maximum values of Q were plotted to show the range of the solution for each cavity. The solution of the problem is the common area between all three sets of lines. It is seen that the correction for side wall loss is not significant in these measurements.



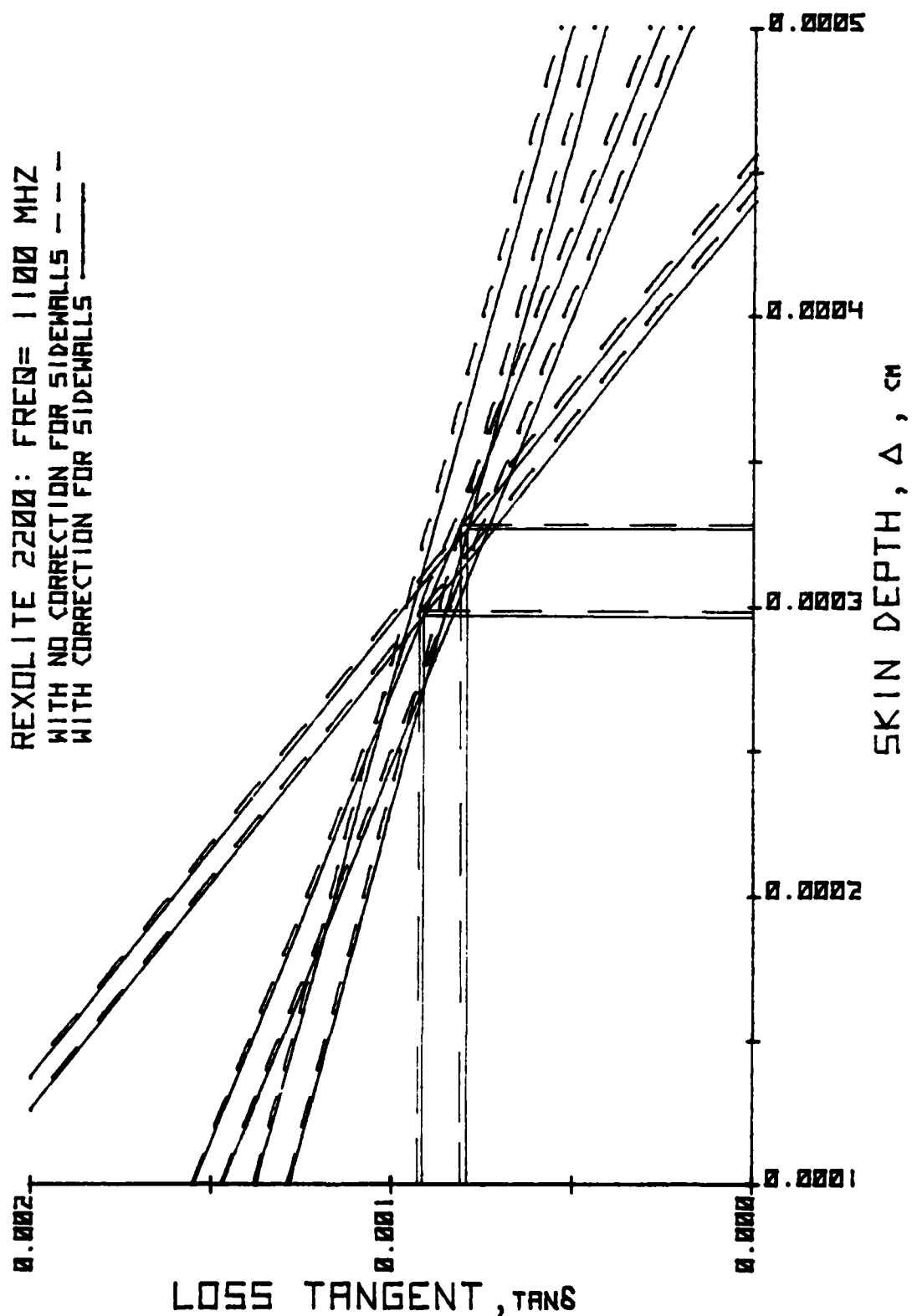


Figure 10 Solution Methods Plot



The plots for separating the loss tangent and skin depth for the frequency range of 600 MHz to 2 GHz are presented in Figure 11a-m. The results of these plots are presented in Table 1.

FIGURE	FREQUENCY MHz	$\tan \delta$	$\Delta$ (cm)
a	605	.00082 - .00097	.0003625 - .00039
b	680	.00097 - .00119	.00028 - .000355
c	760	.00074 - .00086	.000362 - .000385
d	820	.00078	.000366
e	865	.0007 - .00086	.000328 - .0003685
f	920	.001 - .0011	.000287 - .0003135
g	1100	.00091 - .00095	.0003 - .000313
h	1100	.00079 - .00091	.000296 - .000327
i	1365	.00098 - .00104	.000254 - .00027
j	1540	.000825 - .00093	.000268 - .000299
k	1785	.00104 - .00108	.000203 - .00023
l	1940	.00084 - .00087	.000242 - .00025
m	2050	.001 - .00111	.0001865 - .000218

TABLE 1 Solution Results



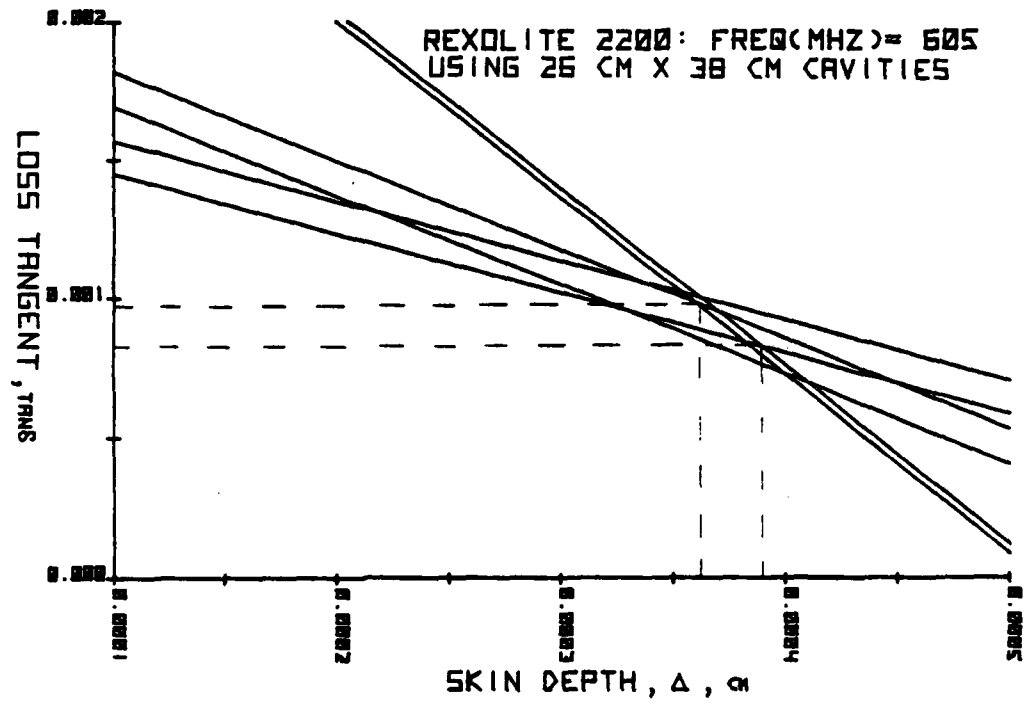


Figure 11a Solution Plot

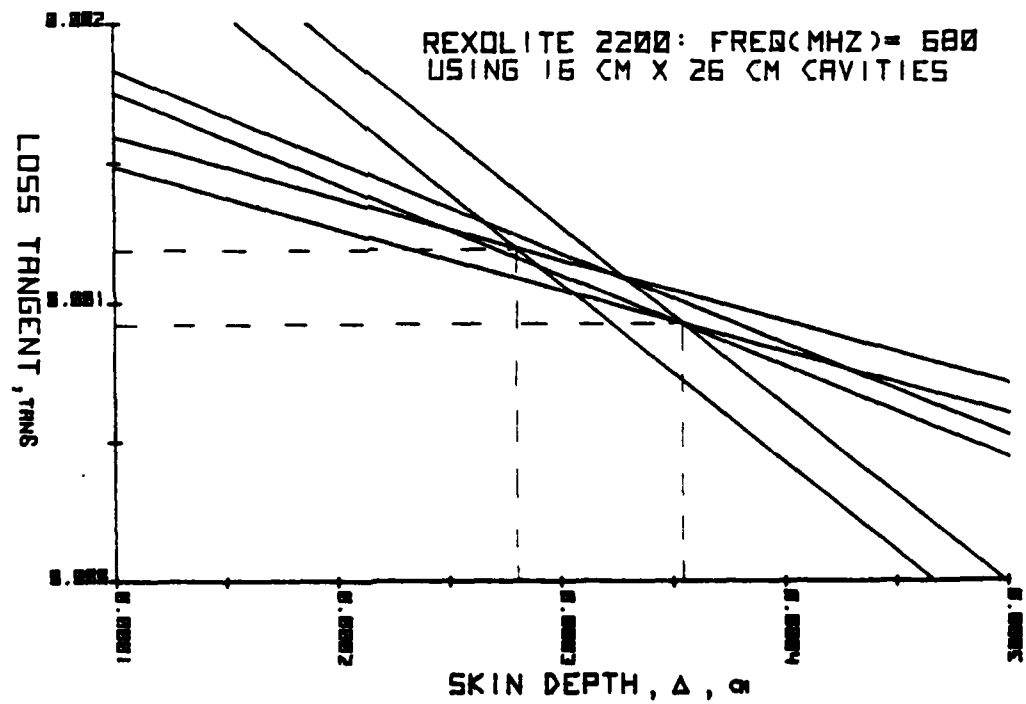


Figure 11b Solution Plot



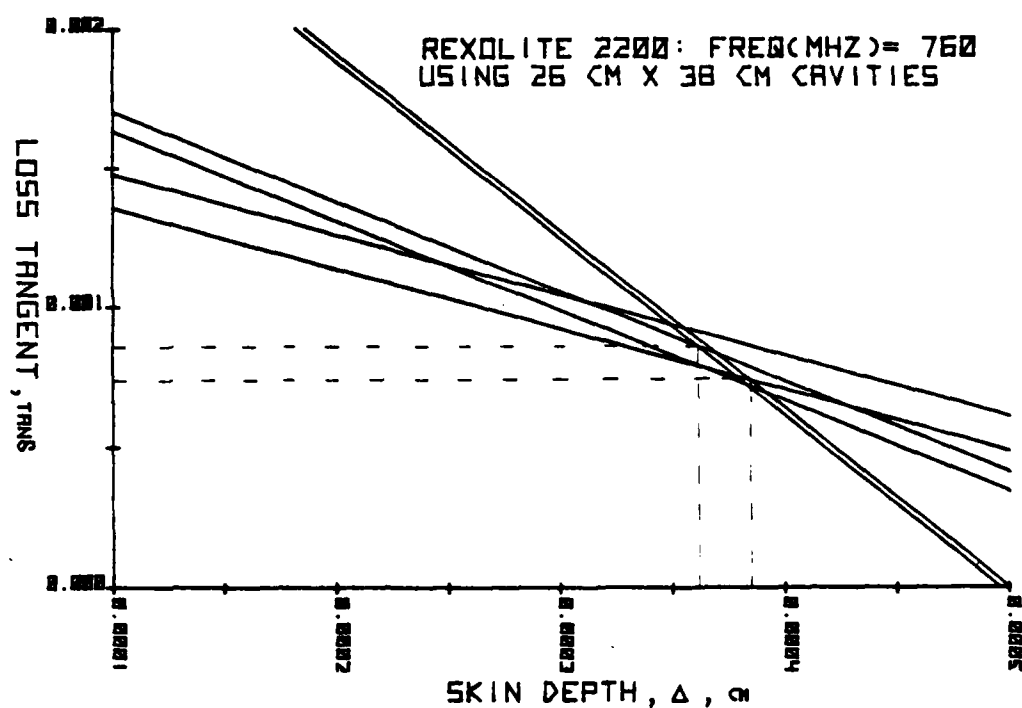


Figure 11c Solution Plot

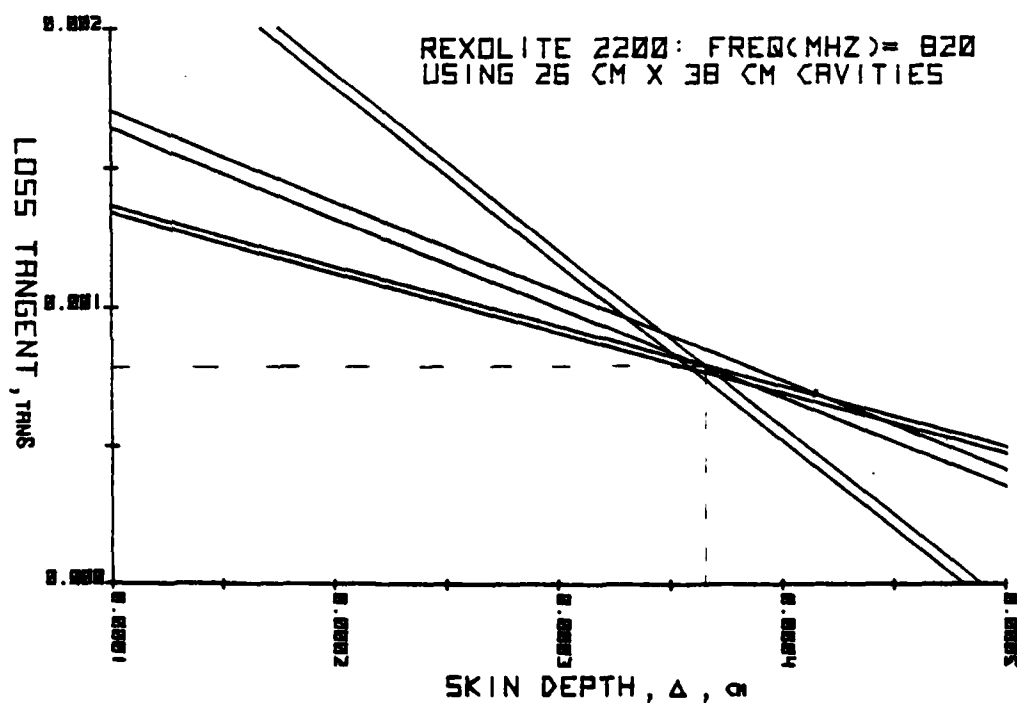


Figure 11d Solution Plot



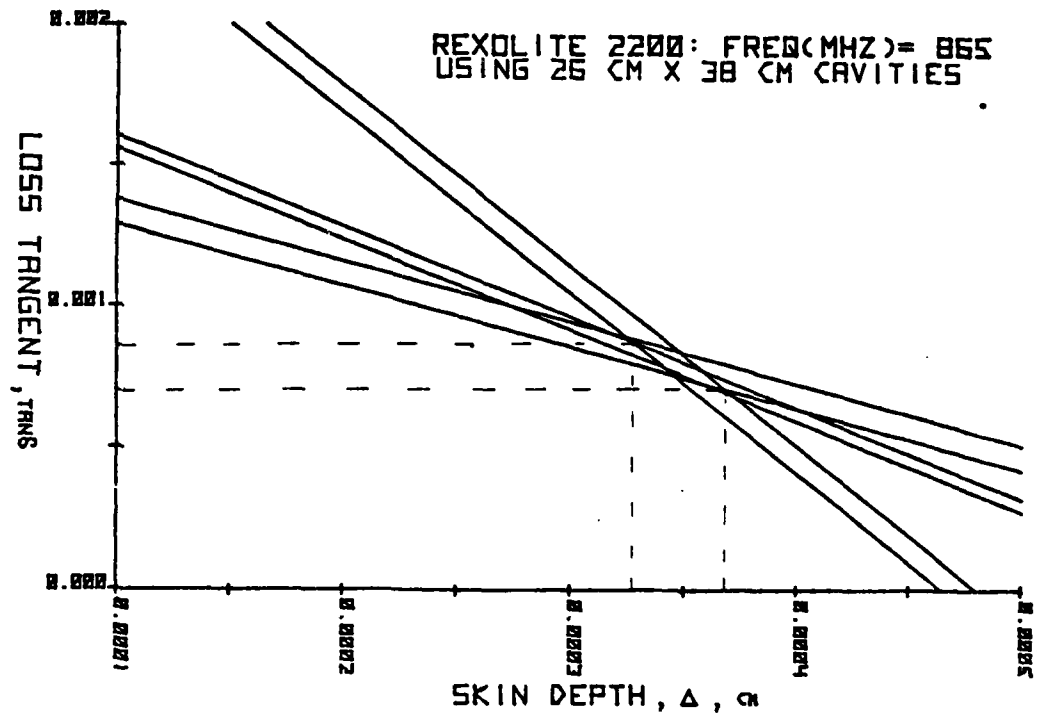


Figure 11e Solution Plot

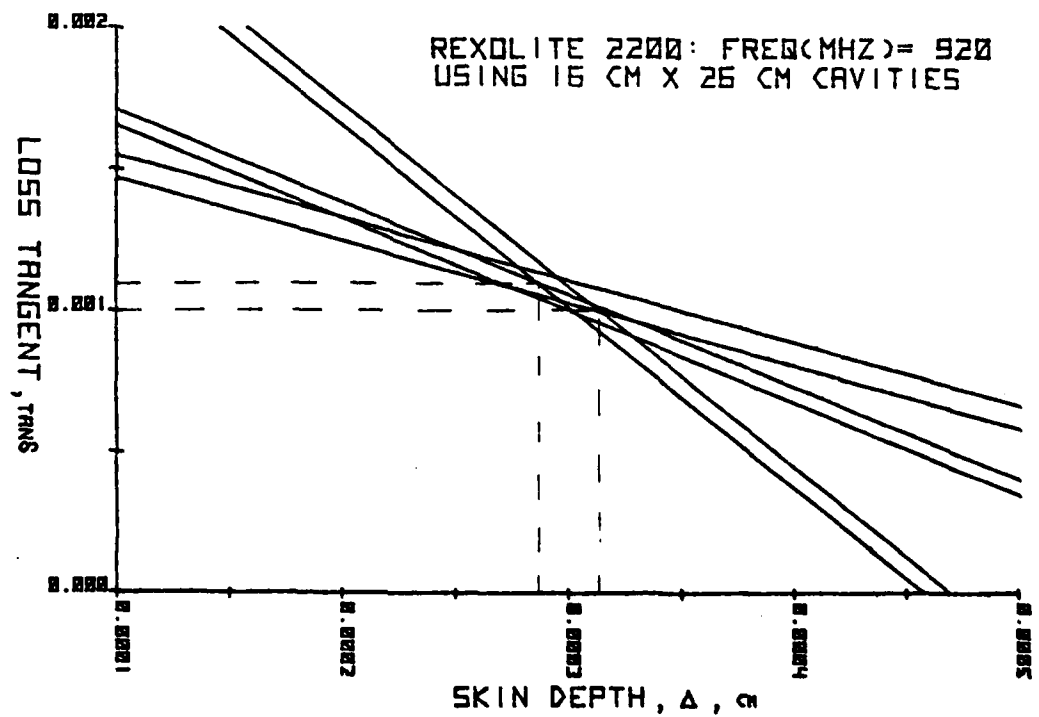


Figure 11f Solution Plot



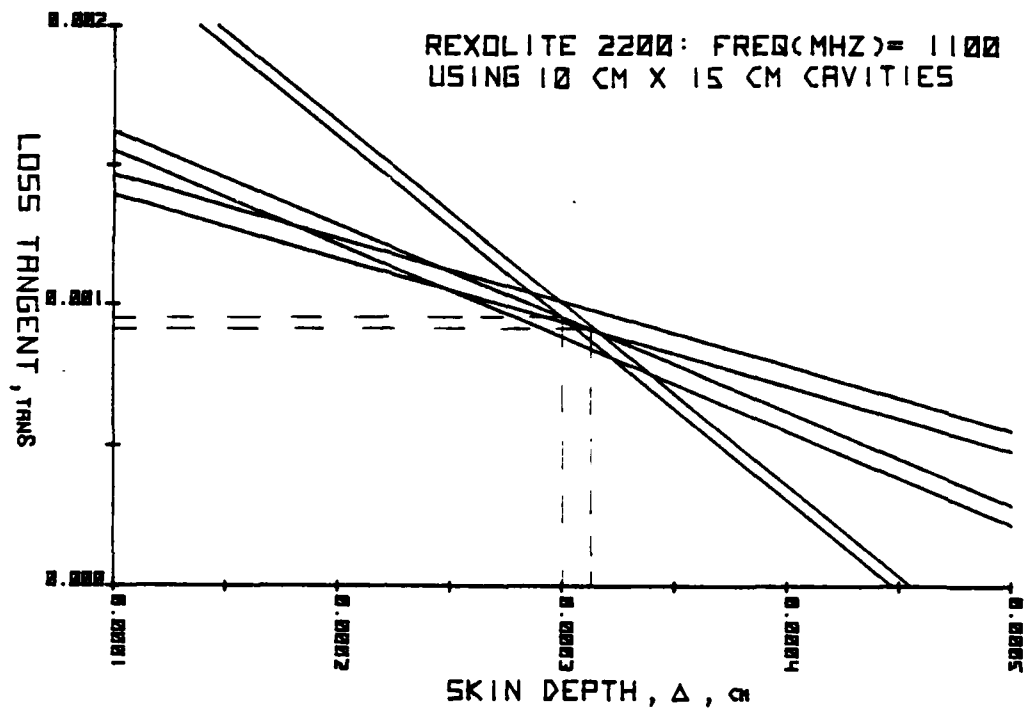


Figure 11g Solution Plot

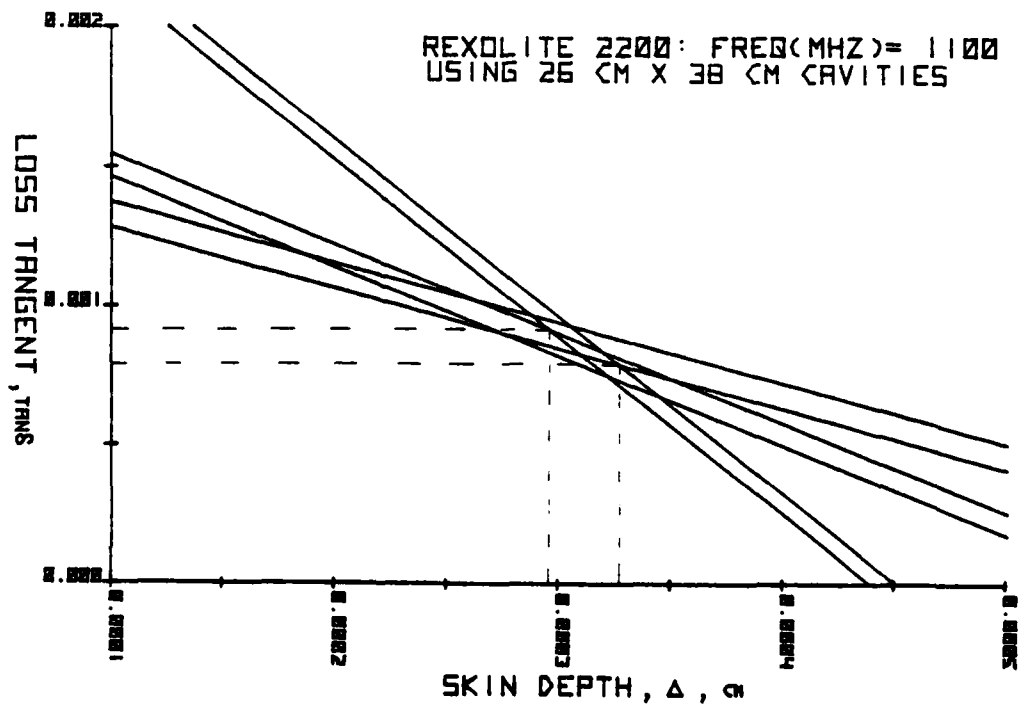


Figure 11h Solution Plot



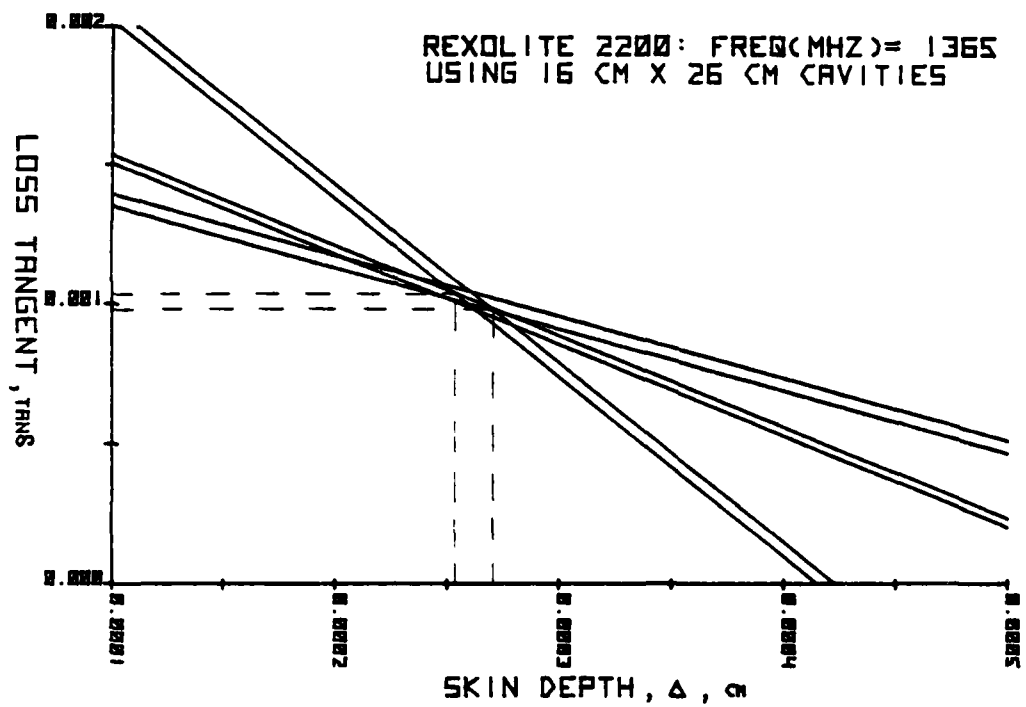


Figure 11i Solution Plot

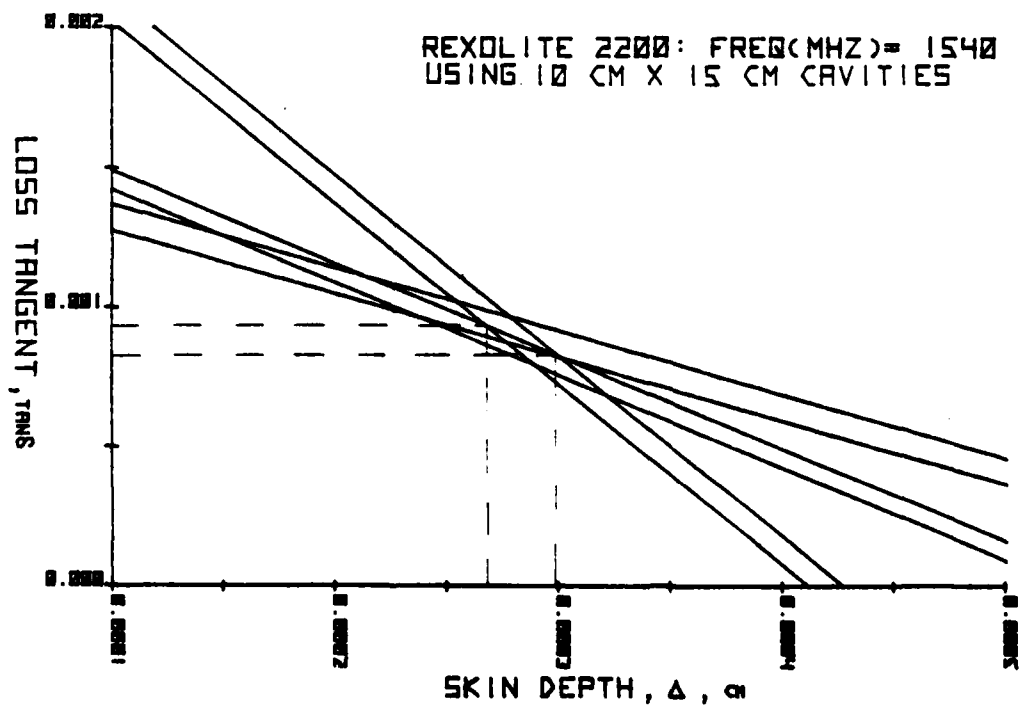


Figure 11j Solution Plot



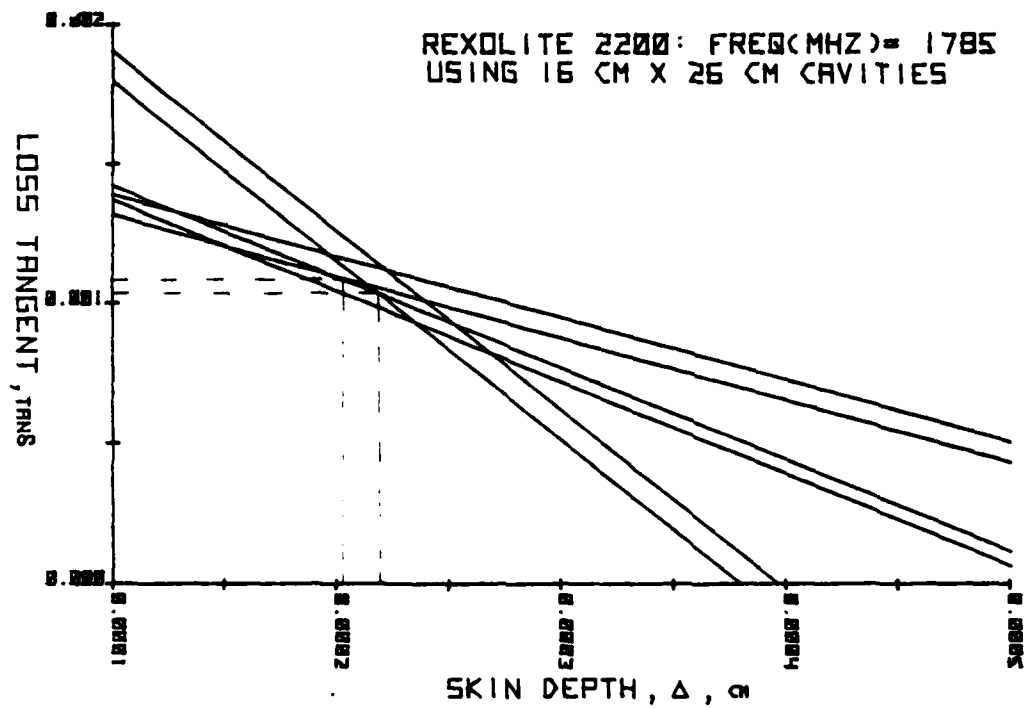


Figure 11k Solution Plot

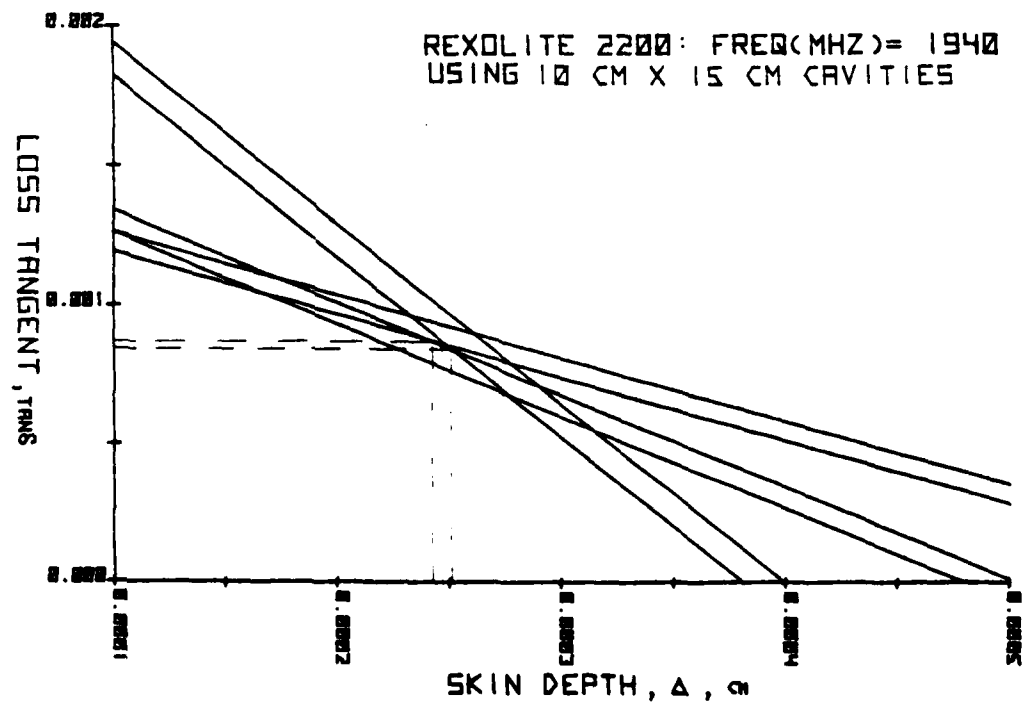


Figure 11L Solution Plot



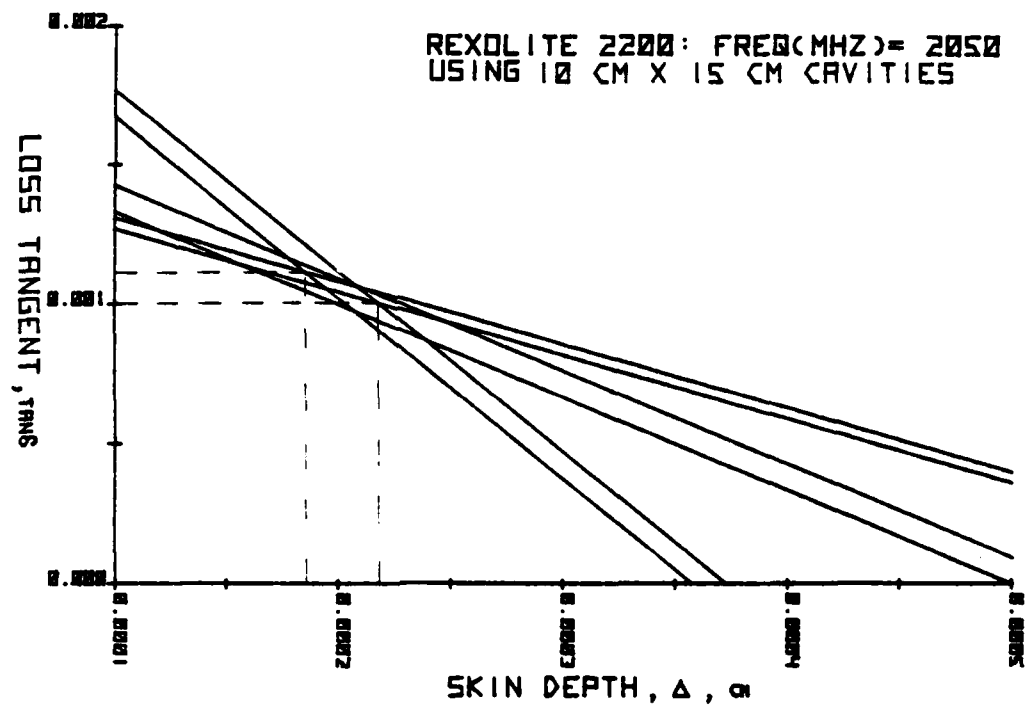


Figure 11m Solution Plot



In general, the loss tangent for the Rexolite 2200 was found to be about .001. The skin depth was found to be about .0038 cm at 600 MHz and about .00022 cm at 2 GHz. The conductivity was then calculated to be about  $2.7 \times 10^7$  mho/meter. The plots of skin depth, loss tangent, and conductivity vs. frequency are presented in Figure 12-14.

Since the conductivity of copper is  $5.8 \times 10^7$  mho/meter this test shows that there is more loss in the copper plates than would be calculated assuming simply copper loss. Therefore this result shows that the bonding agent and the roughness at the copper-dielectric interface have decreased the conductivity by a factor of slightly over 2.

The efficiency of a microstrip antenna can be estimated by the formula relating the losses and the radiation:

$$\frac{1}{Q} = \frac{1}{Q} \text{ radiation} + \frac{1}{Q} \text{ dielectric} + \frac{1}{Q} \text{ copper}$$

Since the Q of a 1/16" antenna is roughly 100

$$\frac{1}{Q} = .01$$

From the above measurements:

$$\frac{1}{Q_{\text{copper}}} = \frac{\Delta}{t} = \frac{.003_{\text{cm}}}{.15875_{\text{cm}}} = .0019$$

$$\frac{1}{Q_{\text{dielectric}}} = \tan \delta = .001$$



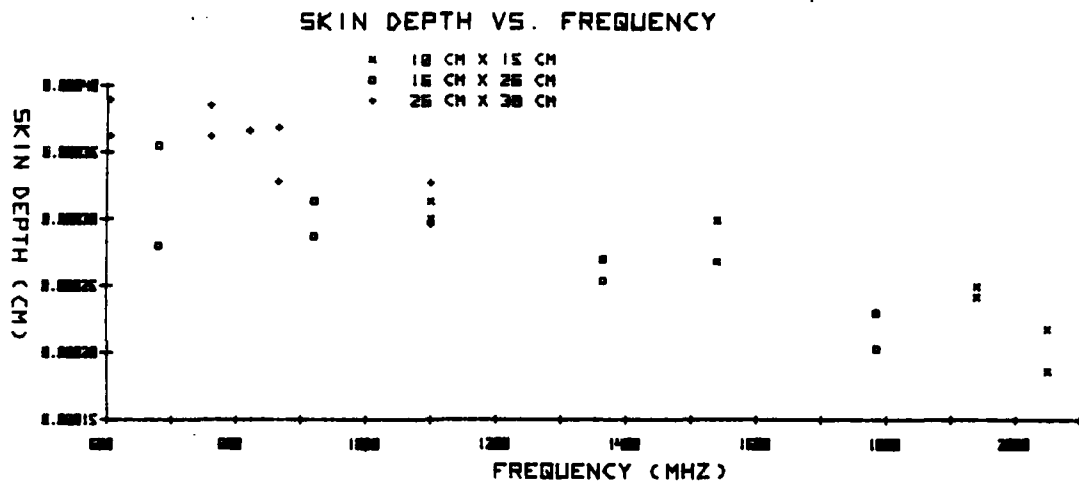


Figure 12 Skin Depth Solution

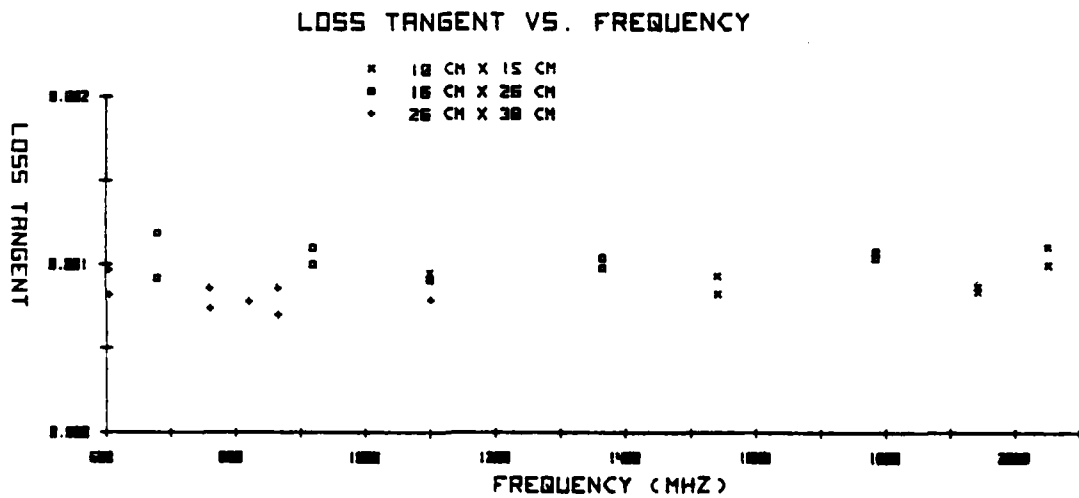


Figure 13 Loss Tangent Solution

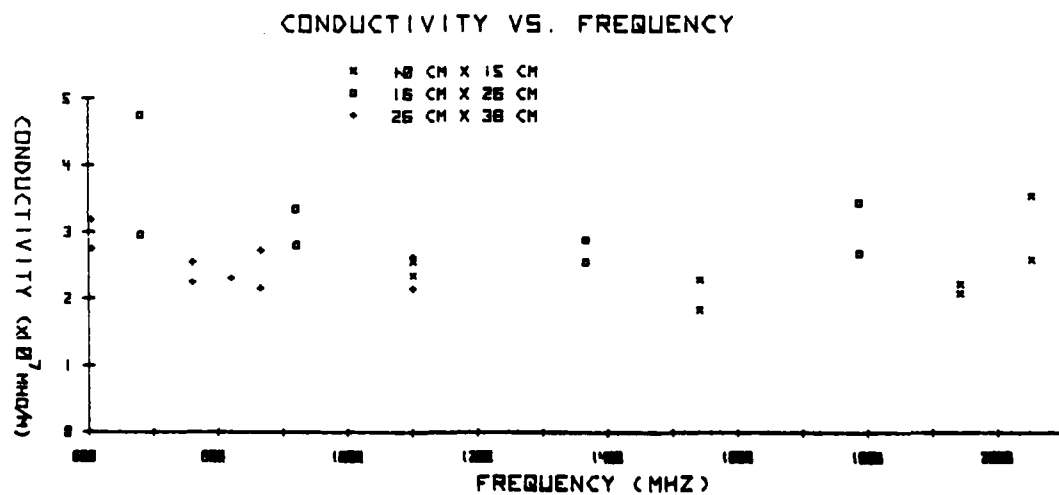


Figure 14 Conductivity Solution



Then

$$\frac{1}{Q} = \frac{1}{Q} \text{ radiation} + .0019 + .001 = 0.01$$

$$\frac{1}{Q} \text{ radiation} \approx .007$$

which shows 70% radiation efficiency for the antenna.

#### B. RESULTS FOR DUROID 5880

Samples of three thicknesses of Duroid 5880 were obtained to test by this procedure. The three thicknesses were .125", .062", and .031". The cavity dimensions were 4.975" by 7.95". The lowest resonant frequency of an empty cavity was found to be:

$$f = \frac{c}{2\pi} \sqrt{\left(\frac{\pi}{a}\right)^2 + \left(\frac{\pi}{b}\right)^2} \quad (4.4)$$

$$= 1.4003 \times 10^9 \text{ Hz}$$

The lowest resonant frequency of this cavity was measured as 943 MHz. Therefore the relative dielectric constant of this sample was found to be:

$$\epsilon_r = \left( \frac{f}{f_{\text{Duroid}}} \right)^2 \quad (4.5)$$

$$= 2.2041$$



The Q was measured at this frequency for the three thicknesses. For the thickest cavity the Q was measured from 532.8 to 563.2, for the middle thickness cavity 405.1 to 429.3, and for the thinnest cavity 254.1 to 286.6.

The plot for separation of loss tangent and skin depth is shown in Figure 15. The solution of this plot shows a loss tangent between .00106 and .00132, a skin depth between .000169 cm and .000218 cm and a conductivity between  $5.67 \times 10^7$  mho/meter and  $9.4 \times 10^7$  mho/meter. The unreasonably high value of conductivity (as compared with that of copper  $5.8 \times 10^7$  mho/meter) is perhaps mainly due to our over-simplified model in evaluating the skin-effect of the complex surface and bonding agent between the copper and the substrate. Nevertheless, this result seems to show that the bonding agent and the copper-dielectric interface are less lossy than for Rexolite 2200. The results for loss tangent are twice as high as the published value, this could be from a bad batch of material or absorbed moisture [5] .



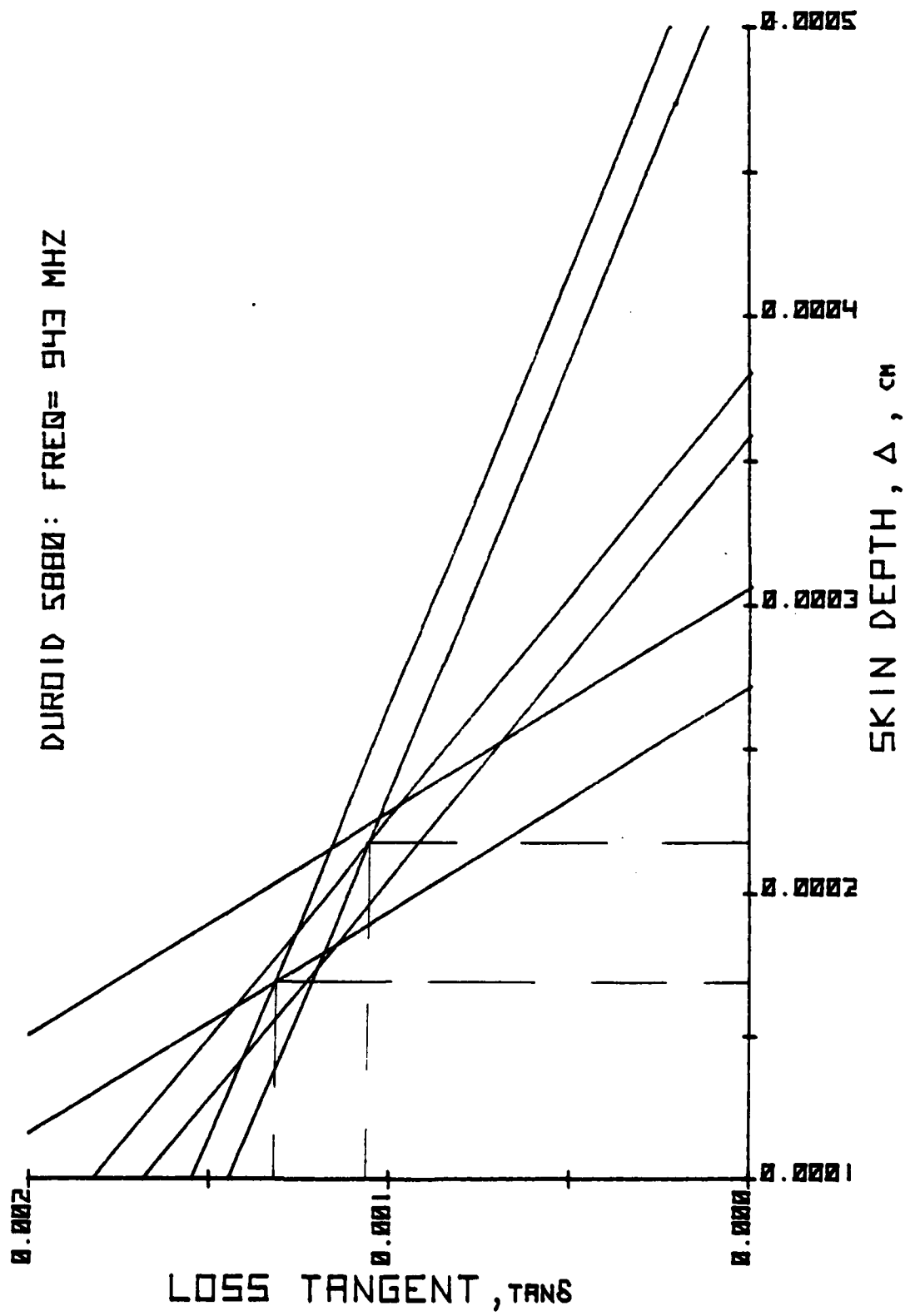


Figure 15 Solution Plot



## CHAPTER 5

## DISCUSSION

## A. SELF CONSISTENCY

Three thicknesses of cavities were used in this study to check for self consistency. The first two cavities determined the solution area and the third cavity, in addition to narrowing the results, confirmed the results.

In Figures 10 and 14 the majority of results had good agreement. The results that had poorer agreement were from cavity imperfections or measurement errors.

In the initial tests of Rexolite 2200 cavities of different thicknesses were not made from multiple layers of a single 1/16" stock. Instead, they were constructed with stocks of different thicknesses. When these results were plotted there was no common area between their characteristic lines. This showed that different batches of Rexolite 2200 have surprisingly large differences in characteristics. This finding was confirmed in literature [4] .



## B. MEASUREMENT ERROR REDUCTION

Measurement errors were reduced by making multiple measurements. Unloaded  $Q_0$  and loaded  $Q_L$  were measured several times. These results gave a 5 to 10 percent range for measured  $Q$ . By using a range of  $Q$  rather than a single value measured, errors from repeatability were reduced.

## C. AIR GAPS

Air gaps between dielectric layers were of concern. In other test methods the air gaps were shown to have an effect. A multi-layered test cavity was used to check for air gap effects. The  $Q$  and resonant frequency of the cavity were measured for increasing gaps between the dielectric sheets. This was accomplished by using clamps to hold the sheets together and then loosening them in steps.  $Q$  varied in a random manner within the repeatability of the previous measurements. The resonant frequency did progressively increase when the gap was increased. This could be explained because the effective permittivity in the cavity is decreased.

It was reasonable that the  $Q$  of these cavities should not change more than the repeatability for small gaps. When the gaps were small the resonant mode was not affected. Since



the amount of dielectric material was not changed the total loss in the dielectric was not changed with the same field in the cavity. Thus, the  $Q$  remained unchanged.

#### D. END WALLS

The end walls were made of copper tape. The smooth side was placed against the dielectric edge and the copper tape was soldered to the edges of the top and bottom copper plates as in Figure 16.

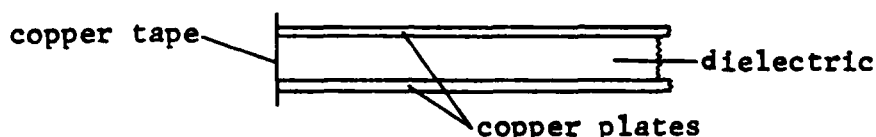


Figure 16 Edge Construction

The copper tape was chosen for convenience and to provide negligible loss in the end walls. There are problems using this tape. One problem is that the tape doesn't lay perfectly flat against the substrate at the cavity edges. The cavity so constructed is not exactly the theoretical model of a perfectly rectangular cavity for the resonant mode. Another uncertainty is the effect of the solder joint



around the edge. There was heat applied at the edge for soldering. The heat was applied carefully but its affect on the material is not known. The sticky side of the tape was not used because the properties of the adhesive were not known and it was hard to solder.

#### E. FEED POINT

The theoretical cavity model and the loss calculations do not include a feed point. The feed used in all cavities was semi-rigid coax fed through the cavity as in Figure 17.

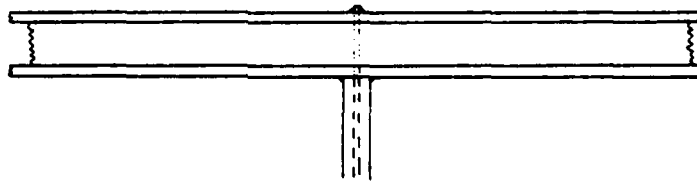


Figure 17 Feed Line

The feed was assumed to have minimal effects on the cavity  $Q$ . This was verified by measuring the  $Q$  of the cavity with the feed at various positions. The  $Q$  measured was within the range of the repeatability of measurement. It was noted that the coupling coefficient changed with different feed points corresponding to varying field intensities in the cavity.



#### F. TIME, MOISTURE, AND TEMPERATURE

There were no tests performed noting moisture content of the air, drying the samples in an oven, or testing samples left out over long periods of time. It was noted in the literature that these dielectrics do change characteristics with changes in moisture content [5] and temperature [2] .

#### G. MODE APPROXIMATION

The calculations of modal fields involved approximating the cavity as lossless. Actually the cavity walls and the dielectric have losses and the true fields may differ. This is another possibility for slight error.

#### H. SOLID CAVITY

A solid cavity was constructed to compare this measurement method to another method. The cavity was made of 1/32" copper sheets and 1/8" copper stock. Q was measured with the cavity filled and empty. Successful measurements of an empty cavity were not possible due to inability to maintain cavity dimensions with no internal support.



## I. REDUCING SOLUTION AREA

The method in this report involves plotting the extreme values of  $Q$ . To reduce the solution area the average value of  $Q$  for each thickness could be plotted as in Figure 18. While these lines do not cross at a single point, they do construct an area that is smaller than the area constructed by the first method. This method may or may not be more accurate.



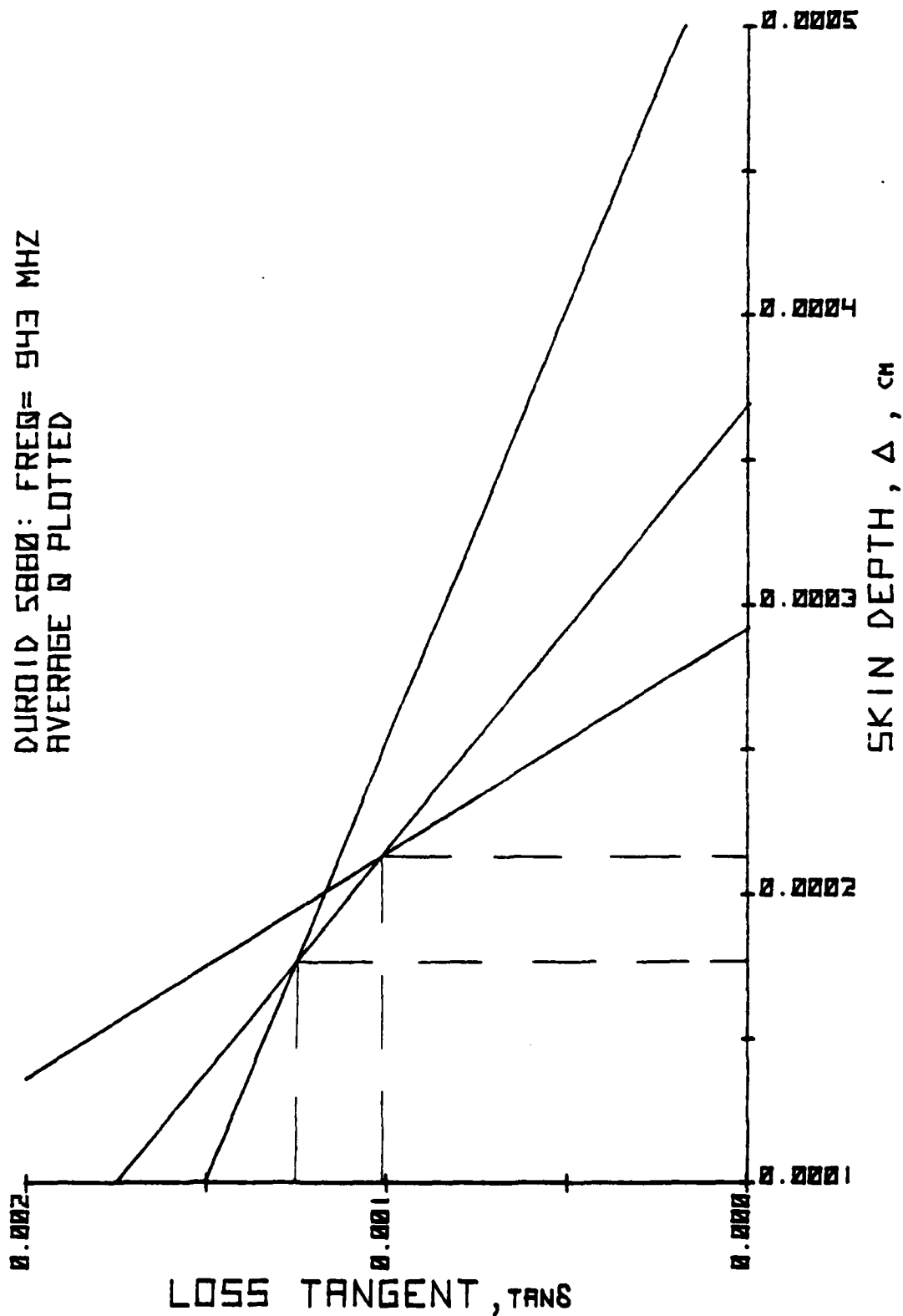


Figure 18 Solution Plot



## C H A P T E R 6

## CONCLUSION

This measurement method is a quick, easy, and inexpensive way to determine what the characteristics of a microstrip antenna material are. As presented it is not a very precise measurement method, but does give useful results for separating the two losses, dielectric and copper.

For future measurements of materials only two cavity thicknesses are required if the samples are from the same stock. For measurements comparing samples of different stocks three thicknesses should be used to confirm similarity of material.



## R E F E R E N C E S

1. Ginzton, E. L., Microwave Measurements (1957 McGraw-Hill Book Company, Inc.)
2. Sucher and Fox, Handbook of Microwave Measurements, Vol. II (1963 Polytechnic Press of the Polytechnic Institute of Brooklyn).
3. Sato, New Method for Measuring Dielectric Properties of Material Media Using Microstrip Cavity, (Thesis, University of Illinois 1973).
4. Howe, Harlan, Jr., "Dielectric Material Development," (Microwave Journal, November 1978), pp 39-40.
5. Olyphant, M., Jr., Demeny, D.D., and Nowicki, T.E., "Epsilon 10 - A New High Dielectric Constant Conformable Copper-Clad Laminate", (CU-Tips, 3M Company)
6. Jordan and Balmain, Electromagnetic Wave and Radiating Systems (1968 Prentice-Hall, Inc. Englewood Cliffs, N. J.)



## A P P E N D I X

To show that the equation  $\bar{B}_n = G_n + 1$  are two straight line segments in the Smith impedance chart as shown in Figure 3a, we first let the normalized cavity admittance be  $Y_n$  and then consider:

$$\begin{aligned}\Gamma &= \Gamma_r + j \Gamma_i = \frac{1 - Y_n}{1 + Y_n} = \frac{1 - (G_n + jB_n)}{1 + (G_n + jB_n)} \\ &= \frac{[(1 - G_n) - jB_n][(1 + G_n) - jB_n]}{(1 + G_n)^2 + B_n^2} \\ &= \frac{(1 - G_n^2) - B_n^2 - j2B_n}{(1 + G_n)^2 + B_n^2} \\ \Gamma_r + 1 &= \frac{(1 - G_n^2) - B_n^2}{(1 + G_n)^2 + B_n^2} + 1 \\ &= \frac{2(1 + G_n)}{(1 + G_n)^2 + B_n^2}\end{aligned}$$

If  $1 + G_n = \bar{B}_n$ , then

$$\Gamma_r + 1 = \pm \Gamma_i$$

which are two straight lines, the first passing through points



$(-1 + j0)$  and  $(0, j)$  and the second,  $(-1 + j0)$  and  $(0, -j)$  in the  $\Gamma$ -plane as shown in Figure 3a. One can show similarly that the equations  $\bar{+}X_n = R_n + 1$  give two line segments  $\pm \Gamma_i = \Gamma_r - 1$  in the  $\Gamma$ -plane. These lines pass through  $(1, j0)$  and  $(0, \bar{+}j)$  respectively.

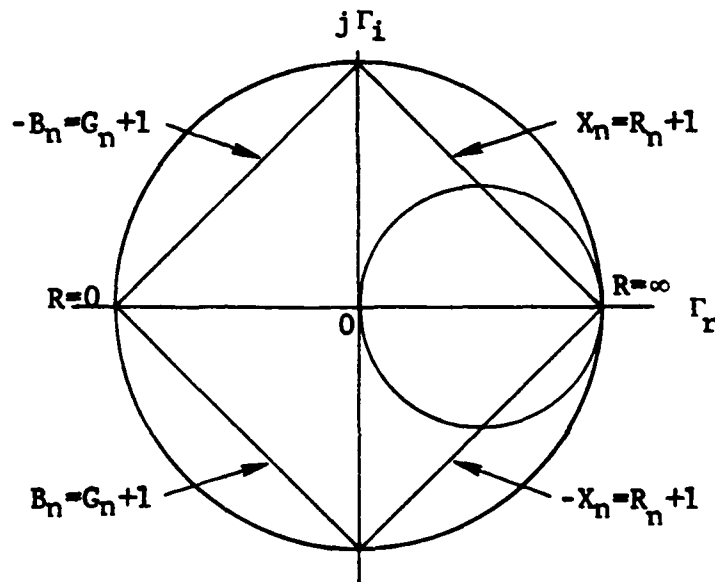


Figure 19  $\Gamma$ -Plane

This shows that the results given in Reference [1], page 409 are incorrect. Since the mapping of  $Z = (R, X)$  to  $\Gamma$  involves, besides translation and scaling, essentially an inversion with respect to a circle of radius 2 and center at  $(-1, 0)$  in the  $\Gamma$ -plane, the lines  $\pm B_n = G_n + 1$ , passing through the center  $(-1, 0)$  will be mapped into lines which are reflections of  $\pm B_n = G_n + 1$  with respect to the real  $\Gamma_r$ -axis. Therefore the above results are expected.





## *MISSION of Rome Air Development Center*

*RADC plans and executes research, development, test and selected acquisition programs in support of Command, Control Communications and Intelligence (C<sup>3</sup>I) activities. Technical and engineering support within areas of technical competence is provided to ESD Program Offices (POs) and other ESD elements. The principal technical mission areas are communications, electromagnetic guidance and control, surveillance of ground and aerospace objects, intelligence data collection and handling, information system technology, ionospheric propagation, solid state sciences, microwave physics and electronic reliability, maintainability and compatibility.*



DATE  
FILMED  
-8